RSI Technical Note TN-026

Measuring Tidal Channel Turbulence with a Vertical Microstructure Profiler (VMP)

Rolf Lueck (Rockland Scientific)

Fabian Wolk (Rockland Scientific), Kevin Black (Partrac Ltd.)

2013-01-15

Rockland Scientific Inc.
520 Dupplin Rd
Victoria, BC, CANADA, V8Z 1C1
www.rocklandscientific.com

1 Executive Summary

The proper assessment of turbulence levels is a key measurement requirement for the successful prediction of tidal-stream energy resources and for the optimization of devices used for the energy conversion. This report introduced an instrumentation solution for direct in-situ measurement of small-scale turbulence, suitable for profiling and mooring application.

This report describes the measurement of turbulence characteristics in Islay and Corryvreckan Sounds on the west coast of Scotland, both of which are locations of future tidal energy power generation. The objective is to demonstrate an instrument system capable of providing high resolution turbulence profiles over the full depth of the water column, even during peak currents of a spring tide.

The data were collected with the Vertical Microstructure Profiler, VMP-200, which is a free-fall profiler that is widely used in oceanographic research. The VMP-200 measures two components of the vertical shear of horizontal velocity over scales as small as 0.003 m. The VMP also carries two thermometers that resolve temperature variations over scales of 0.007 m with a detection limit of 20 µ°C, and ancillary sensors to measure pressure, vibrations and inclination. The vertical shear $(\partial u/\partial z, \partial v/\partial z)$ is used to estimate the rate of dissipation of turbulence kinetic energy, and to provide the two horizontal components of the turbulence velocity fluctuations (u', v'). The temperature measurements provide both the large-scale thermal structure, the size of overturning eddies, and the turbulence fluctuations of temperature.

Measurements were taken over all phases of the tide in currents as strong as $4\,\mathrm{m\,s^{-1}}$. Twenty-two full-depth profiles were taken in the Gulf of Corryvreckan , nineteen in Islay Sound, seven in the Strait of Jura. The data were collected over two and one-half days of daylight operations. The large-scale velocity field was measured concurrently with a ship-side mounted 600 kHz acoustic Doppler current profiler.

The data have been processed with proprietary processing routines developed by Rockland Scientific. The outputs are relevant to CFD and tidal blade numerical models, providing direct measurements of turbulent kinetic energy and dissipation (k and ϵ), quantities which usually are approximated using theoretical arguments or estimated from large-scale current measurements. In addition, the ease of deployment provided by the VMP demonstrates the suitability of this type of instrument for the rapid assessment and monitoring of turbulence parameters at tidal energy sites.

Contents

List of Figures

2 Background

This section provides a short background on vertical free-fall profiling, the shear probe sensor that is used to detect vertical shear on scales of $O(0.001 - 1\,\mathrm{m})$ scales, the estimation of the rate of dissipation of turbulent kinetic energy, and the turbulence parameters that can be derived from measurements taken with a vertical profiler.

2.1 What is turbulence

There is no formal definition of turbulence. Instead, it is described as a syndrome with key characteristics, which together, distinguish it from non-turbulent fluid motions. The key characteristics are [1];

- The flow is chaotic or highly irregular or random.
- The flow is rotational – it has three-dimensional vorticity.
- The flow is dissipative – kinetic energy is irreversibly lost through friction.
- The flow is diffusive – causing rapid mixing of fluid properties such as momentum, heat, and other scalar properties.
- The flow is non-linear and transports energy from large-scale eddies to small-scale eddies.
- The flow has a high Reynolds number.
- Turbulent flows are a continuum – the size of the smallest eddies is still many of factors of 10 larger than any molecular length scale.

Turbulence is a characteristic of a *flow* and not of a *fluid*. There are non-turbulent flows that have some but not all of the above-listed characteristics. For example, surface waves can be highly irregular but the water motion induced by surface gravity waves is irrotational. Surface waves are highly linear until they grow to the verge of breaking. Then, they can induce considerable turbulence into near-surface water.

The starting point for all analytic treatments of turbulence are the Navier-Stokes equations. If the flow is statistically stationary, velocity and scalar quantities can be decomposed into the sum of a mean value and a zero-mean fluctuation – the Reynolds decomposition. The kinetic energy of the turbulence, in a unidirectional vertically sheared flow, is then described by [2]

$$-\overline{u'w'}\frac{\partial U}{\partial z} = \epsilon + \frac{g}{\rho}\overline{\rho' w'} \tag{1}$$

where the Reynolds stress, $-\overline{u'w'}$, working against the mean vertical shear, $\partial U/\partial z$, is the rate of production of turbulence kinetic energy and equals the rate at which it is extracted from the mean kinetic energy of the flow. The rate of production is balanced by the thermodynamically irreversible loss to molecular friction, ϵ, and the upward flux of of potential energy, $g\overline{\rho' w'}/\rho$, where g is gravity and ρ the density of the fluid. The rate of dissipation of TKE is

$$\epsilon = \frac{1}{2}\nu \overline{\left(\frac{\partial u_i}{\partial x_j} + \frac{\partial u_j}{\partial x_i}\right)\left(\frac{\partial u_j}{\partial x_i} + \frac{\partial u_i}{\partial x_j}\right)} \tag{2}$$

where we use summation over repeated indices and ν is the kinematic viscosity [1]. In isotropic turbulence the rate of dissipation can be derived from any shear or rate-of-strain term because (2) then reduces to

$$\epsilon = \frac{15}{2}\nu \overline{\left(\frac{\partial u}{\partial z}\right)^2} = 15\nu \overline{\left(\frac{\partial u}{\partial x}\right)^2} \tag{3}$$

The potential energy flux is usually negligible in a well-mixed tidal channel resulting in a direct balance between the the rate of production and the rate of dissipation of TKE. Measuring the rate of production is difficult because it requires the simultaneous measurement of the Reynolds stress (which itself is very difficult) and the mean vertical shear. The turbulence profiler described in this report measures, ϵ, the rate of dissipation of TKE – the fundamental parameter relating the loss of energy in the flow to the turbulent stress and shear.

Because the density stratification in a tidal channel is usually weak, the turbulent velocity fluctuations are nearly isotropic (independent of direction) which means that the variance of individual components are equal,

$$\overline{u'^2} = \overline{v'^2} = \overline{w'^2}, \tag{4}$$

and that the variance of the total fluctuating velocity

$$q^2 = \overline{u'^2} + \overline{v'^2} + \overline{w'^2}, \tag{5}$$

can be derived from any single component. The length scale of turbulent eddies, l is related to the velocity and the rate of dissipation by

$$q^{3/2} = \epsilon l. \tag{6}$$

2.2 Taylor Frozen Field Hypothesis

Turbulence is inherently a spatial phenomenon – a cascade of eddies with three-dimensional vorticity that interact to pass energy from the largest scale of a flow down to the smallest scale where the energy is converted to heat by molecular friction. In this process, the fluid is mixed (homogenized), and momentum is transferred towards the (bottom) boundary. The eddies evolve with time but this evolution is slow compared to the time of rotation of an eddy. All theoretical work on turbulence is based on its spatial- and wavenumber-structure.

The time-series of a profile through a turbulent fluid, and the frequency spectra that are derived from a profile, are converted into a space-series and wavenumber spectra using the

"Taylor Frozen Field Hypothesis". The notion is that the time series of any turbulence quantity can be converted into a spatial sequence using

$$g(t) \longrightarrow g(z = Wt) \tag{7}$$

and any time rate-of-change of a turbulence quantity can be converted into an along-path gradient using

$$\frac{\partial}{\partial t} = W \frac{\partial}{\partial z}, \tag{8}$$

where W is the speed of profiling in direction z. The transformation from the time- to the spatial-domain only makes sense if the spatial structures do not evolve during the time interval of profiling. Hence, the assumption of "Frozen Field". The time-scale for the evolution of an eddy of size l is $(l^2/\epsilon)^{\frac{1}{3}}$ (see [3] for an in depth discussion). The VMP profiler measures scales as large as $l \sim O(1\,\mathrm{m})$ and using a very large dissipation rate of say, $\epsilon = 1 \times 10^{-3}\,\mathrm{W\,kg^{-1}}$, gives a time scale of 10 s. However, it takes the profiler only 1 s to traverse this distance, because $W \approx 1\,\mathrm{m\,s^{-1}}$. Thus, the velocity field is effectively frozen, and its time series is accurately transformed into a space series, for features with scales $l \lesssim 1\,\mathrm{m}$.

2.3 Microstructure profilers

A microstructure turbulence profiler is a standard instrument used by the oceanographic research community for the measurement of oceanic microstructure turbulence. Microstructure in this context is defined as the spatial scales where turbulent velocity fluctuations are damped out by the fluid's molecular viscosity, and this range is typically $O(0.001 - 1\,\mathrm{m})$. The turbulence profiler consists of a cylindrical pressure tube with the turbulence sensors mounted on a cone-shaped end cap at the bottom of the tube. They move axially through the water and are propelled by gravity. The measurements are typically made during the downcast, with the sensors positioned on the bottom so that they measure undisturbed water.

Microstructure profilers are widely used to quantify mixing and turbulence for studies in climate change, deep-sea circulation, coastal processes. The development of such profilers began in the 1960s under the leadership of Cox [4] at the Scripps Institute of Oceanography. Other research groups around the globe followed this lead and developed a great variety of vertical profilers, often with unique designs that were geared towards a specific scientific purpose. The first commercially produced instruments became available in the early 2000s. A detailed account of the development of this technology is given in [3].

2.4 The airfoil shear probe

The primary sensor for the measurement of turbulence is the shear probe (Figure 1) which consists of a piezo-ceramic element, 13 mm long, 1.6 mm wide, and 0.5 mm thick, that is embedded halfway into a hollow stainless steel support sting. The free end of the piezo beam is encased in a flexible, bullet-shaped, silicone rubber tip that forms an axially symmetric airfoil.

As the probe moves axially through the water at the speed W (which is the fall-rate of a profiler), the horizontal component of the turbulence velocity, u, turns the total velocity, U, into the vector sum of W and u, and induces an angle-of-attack (AOA), α (Figure 1). When the total velocity has an AOA, it induces a lift force over the surface of the probe, and this force bends (microscopically) the piezo-ceramic beam. The bending of the ceramic liberates or absorbs an electric charge (depending on the direction of bending) and this charge is turned into a voltage, $e = SWu$, where S is the sensitivity of the probe [1] This voltage is time-differentiated to produce the signal $E = \partial e/\partial t = SW\partial u/\partial t$. With the Taylor "frozen field" hypothesis (8), the time rate-of-change of u is converted into a spatial gradient, to yield the vertical shear of horizontal velocity,

$$\frac{\partial u}{\partial z} = W^{-2}S^{-1}E. \tag{9}$$

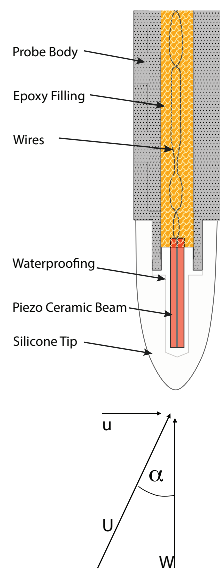

Figure 1: A schematic representation of the air-foil shear probe. With the mean flow, W, primarily axial, a cross-stream perturbation of velocity, u, generates a total velocity, U, with an angle-of-attack, α. This generates a lift force over the surface of the probe, which causes a microscopic bending of the piezo-ceramic beam and generates an electric charge.

The shear probe is sensitive to only a single component of velocity – the component oriented at right angles to the probe axis and normal to the wide surface of the piezo beam. Therefore, two shear probes in parallel, with one rotated by 90° around its axis, can provide both components of vertical shear, $\partial u/\partial z$ and $\partial v/\partial z$. When the shear probe is used in a horizontal

[1] Details of the calibration procedure can be found in [Lueck, R. G., 2010: Converting Shear Probe, Thermistors and micro-conductivity signals into physical units, Technical Note, Rockland Scientific International Inc. TN-005, available at www.rocklandscientific.com] and [5].

configuration (such as towing, or on a glider or AUV, or on a fixed platform in a horizontal flow), the probe measures two components of the horizontal shear, namely $\partial w/\partial x$ and $\partial v/\partial x$, where x is the quasi-horizontal direction of profiling.

The maximum permissible angle-of-attack has not been formally determined, either by observation nor by theory. At some large angle α, the flow over the probe must separate on its lee side and this will impart a change of sensitivity and erratic output. It is commonly assumed that α should be less than 20°. For the last 7 years, RSI has been calibrating the probe for $\alpha = \pm 10°$ in steps of 2°. Prior to that, over the range of $\alpha = \pm 20°$ in steps of 3°. Neither an irregular output, nor a change in slope of output were ever observed. So, the "limit" of 20° is conservative and the actual limit remains unknown.

The shear probe has a finite size and this limits the shortest scales that it can resolve. Various cut-off wavenumbers, and in various mathematic forms, have been suggested over the past few decades, without actual calibration of the wavenumber response. The wavenumber response and its mathematical form have now been established. This was achieved by towing four closely spaced shear probes, where one pair was have the size of a normal probe, through a vigorously turbulent tidal channel. The ratio of the spectra of normal and small probes provides both the cut-off wavenumber of each probe and its analytic form [6]. The shear probe acts as a spatial filter that attenuates the shear spectrum by the factor

$$H(k) = 1 + \left(\frac{k}{k_0}\right)^2 \tag{10}$$

where $k_0 = 48\,\mathrm{cpm}$. The cut-off is equivalent to a spatial resolution of 0.003 m, by the usual definition of spatial scale, namely $l = (2\pi k_0)^{-1}$.

The shear probe was originally developed for wind tunnel measurements [7, 8] in the 1960s and adapted for oceanic measurements [9] in the early 1970s. It soon became, and still is, the exclusive sensor for the measurements of oceanic velocity turbulence, in all regions where it is impossible to rigidly mount an instrument. Acoustic and mechanical sensors are used to measure turbulence close to the bottom, and on the underside of thick ice, where they are mounted on rigidly fixed platforms. The shear probe is used at all depth and in all oceans. It has been mounted on vertical profilers, autonomous underwater vehicles (AUVs), gliders, towed vehicles, submarines, moorings, and even on expendable instruments. A complete list of publications that use data collected with the shear probe would add 30 pages to this report. The review article [3] and the comprehensive text on ocean turbulence [10] are good starting points for further reading on the shear probe.

2.5 Other microstructure sensors

Scalar properties are frequently measured to provide additional insight into ocean turbulence The FP07 thermistor (Figure 2(a)) is commonly used to measure temperature because it has the fastest response of any thermistor-type sensor. The VMP-200 can carry two FP07 temperature sensors. The actual frequency response of the FP07 thermistors is vague. The sparse research literature is inconclusive and estimates range from 12 to 30 Hz [11, 12, 13].

Regardless of the actual value of the frequency response, no temperature sensor can resolve the full spatial range of the fluctuations of temperature in a tidal channel. However, the FP07 thermistor is still useful – turbulent velocity, occurring within a background of a vertical temperature gradient, must generate fluctuations of temperature, and this provides additional information, such as the the vertical size of overturns.

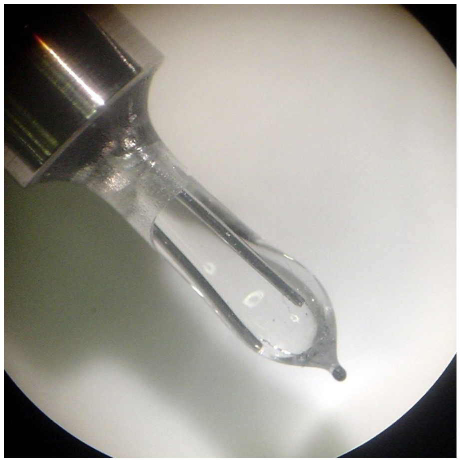

(a)

(b)

Figure 2: (a) Photograph of the FP07 thermistor mounted into a sting suitable for use on the VMP-200 profiler. The tiny, dark-grey, dot in the bottom left corner is the thermistor. It has an outer diameter of 180 µm. The metal oxide of the thermistor is coated with a 5 µm layer of glass. The thermistor is usually mounted adjacent to the shear probes. (b) Photograph of a two-electrode micro-conductivity sensor. The two "needles" are separated by 0.001 m.

A two-electrode electrical conductivity sensors is also used. It can resolve fluctuations with wavelengths smaller than 0.01 m and provides better spatial resolution than the FP07 thermistor. The electrical conductivity of seawater is determined by both temperature and salinity. In open ocean conditions, the contribution of temperature fluctuations towards the fluctuations of conductivity greatly exceeds the contribution from salinity fluctuations. Consequently, electrical conductivity fluctuations are usually interpreted as temperature fluctuations. However, in coastal regions, where the input of fresh water is large, the fluctuations of electrical conductivity are usually dominated by the contribution from salinity. In addition, salinity is usually the most important determinant of density, in coastal regions. Therefore, a micro-conductivity sensor can provide information on the scale of density inversion wrought by turbulence. The VMP-200 can support one micro-conductivity sensor, but no such sensor was installed for the data reported here.

3 The VMP-200 Turbulence Profiler

In this study we used the VMP-200 vertical profiler (3), which carries two shear probes, two high-resolution temperature sensors (thermistors) and a number of ancillary sensors, such as accelerometers, tilt sensors, and a pressure transducer. The VMP-200 is designed for coastal and shelf-region operation. Data are recorded internally on a memory card and downloaded after a sequence of measurements. The VMP-200 is approximately 1.5 m long, has a diameter of 0.1 m, and weighs 120 and 33 N in air and water, respectively.

Figure 3: The VMP-200 mounted into its deck holder with the sensors facing the camera. The four prongs are guards protecting the two shear probes and thermistors mounted on to the bottom end of the profiler. The drag brushes are the white plumage at the top end. The tether-line is the blue cordage laying on deck.

(a) (b)

Figure 4: (a) The VMP-200 about to be tossed into the water, nose first, during a night-time demonstration by Tracey Kutney, Natural Resources Canada, and (b) moments later, with the drag brush still visible.

The VMP is deployed from a drifting ship in a "tethered free-fall mode", where the profiler is connected to the ship by a cable or line that is paid out fast enough to maintain 5 or 6 m of slack near the surface. The fall speed is then fairly constant and independent of ship motions. Brushes at the top end of the profiler provide drag, slowing the profiler to a constant fall speed of $1.0\,\mathrm{m\,s^{-1}}$. Righting moment for the profiler comes from both the separation of its centres of mass and buoyancy, and from the drag of the brushes. The fall-rate is adjusted by changing the number and the size of the brushes.

During the profile, the ship typically drifts with the current and it may be pushed by the wind. The profiler is launched from the upwind side so that the wind pushes the ship away from the loose near-surface tether to reduce the chance of snagging it beneath the ship. Because the deployment ship is allowed to drift, the profiler never experiences the full thrust of the tidal current. Both the ship and the profiler move with the current. However, the large-scale vertical shear of the current will separate the profiler from the ship horizontally in proportion to the ratio of shear to fall-rate. The operator must deploy line quickly enough to satisfy both this horizontal separation and the fall-rate. The windage of the ship adds (vectorially) to the horizontal separation of the profiler from its deployment ship.

The length of a vertical profiler is not chosen arbitrarily and its choice is based on two considerations. The profiler must be long enough to provide an adequate separation of its centres of mass and buoyancy. In addition, the profiler acts as a high-pass filter to the vertical variations in horizontal velocity. A depth-independent horizontal velocity merely translates the profiler sideways and a velocity sensor attached to the profiler cannot detect any horizontal current. When the horizontal current varies with depth, and with scales much larger than the length of the profiler, the profiler will report a much reduced horizontal current, because it will tend to equilibrate with the horizontal current. Only when the scales of the vertical variations are comparable to, and smaller, than the length of the profiler, will a velocity sensor (mounted on the profiler) properly report the environmental current. We want to detect shear on scales of $O(1\,\mathrm{m})$, and smaller, and this requires a profiler that is longer than this value.

The fall-rate of the VMP-200 is determined from its rate-of-change of pressure. Fall-rate variations are less than 1 % in quiescent regions where the vertical velocity of the water is small compared to the fall-rate of the profiler. When the environment is vigorously turbulent, there will be regions of strong up- and down-drafts. The rate-of-change of pressure still gives an accurate measure of the vertical speed of the profiler relative to the surface (or any earth-fixed coordinate system). However, interpretation of the signals from the shear probe requires a measure of the mean axial (vertical) flow past the instrument (9), and this speed can be significantly different from that inferred from the rate-of-change of pressure. An extreme example is an updraft of speed $1\,\mathrm{m\,s^{-1}}$, which equals the nominal fall-rate of the profiler. A profiler in this up-draft would merely hold depth $\partial P/\partial t = 0$. However, water is still streaming past the instrument, and the shear probe signal can still be interpreted using $W = 1\,\mathrm{m\,s^{-1}}$ in (9).

Tests in quiescent waters indicate that the VMP-200 adjusts rapidly from a standing start to its terminal velocity. The profiler reaches 90 % of terminal velocity in less than one body length. This means that the fall-rate, relative to the local water is fairly constant, and variations in the rate-of-change of pressure give a quantitative measure of vertical velocity of eddies that are larger than one body length. The fall-rate of the VMP-200, as configured for the work reported here, was "calibrated" with two 60-m profiles taken in fairly quiescent waters in the Sound of Jura during slack tide.

4 Turbulence Parameters derivable from a VMP

A vertical turbulence profiler, such as the VMP-200 can provide the data to derive the following list of turbulence parameters.

- Profiles of the rate of dissipation of TKE.
- Profiles of two orthogonal components of horizontal turbulence velocity.
- Profiles of temperature and hence, the overturning scale of eddies.
- The rms-velocity of overturns using $q = (\epsilon l)^{2/3}$ where l is the vertical length scale of overturns (6).
- The wavenumber spectrum of shear and horizontal velocity over selected depth ranges.

5 Islay Sound Data

A typical example of the turbulence information provided by the VMP-200 is exemplified by profile DAT_008_4. This profile was taken in Islay Sound (Figures 5,6) at 2012-10-13 13:02 UTC, within less than 1000 m of the ferry terminal, where the channel is approximately 65 m deep. The profile was terminated 10 m above the bottom. The near-spring tidal flood (flow towards the open sea) was close to its peak of $3\,\mathrm{m\,s^{-1}}$. The following sub-sections describe the VMP data in detail.

Figure 5: Islay Sound looking north with Islay and Jura islands left and right, respectively. The ferry terminal is in the white structures on the left.

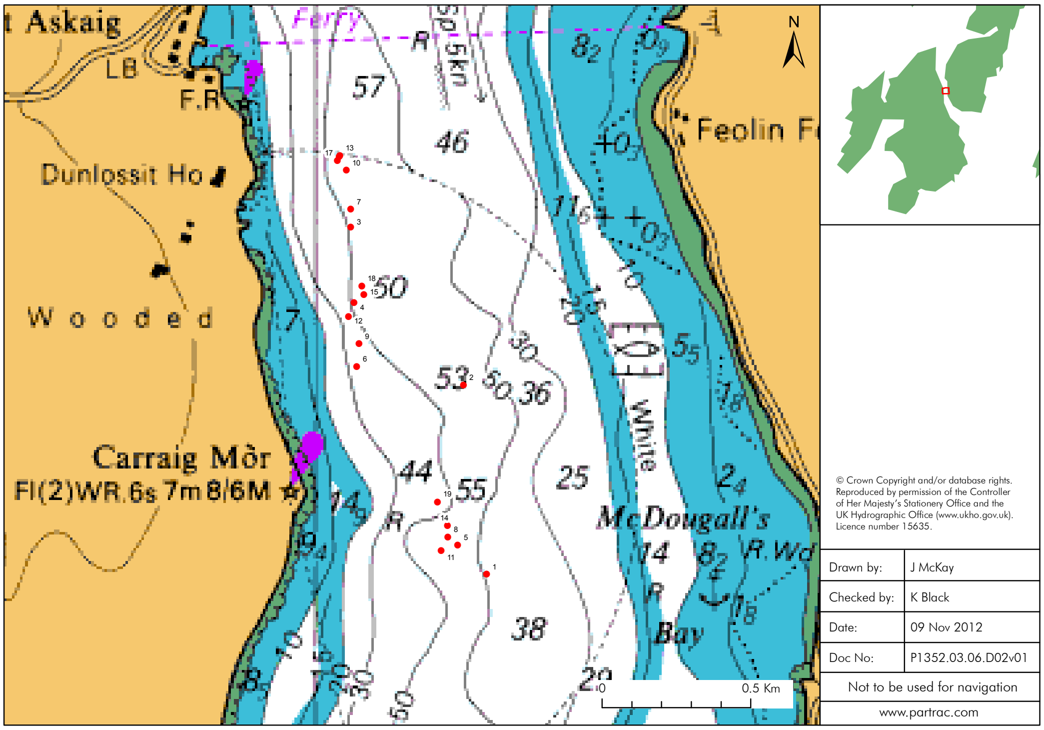

Figure 6: The location (red dots) of the VMP-profiles take in Islay Sound on 2012-10-13.

5.1 Basic Kinematic Behaviour

The fall-rate of the profiler quickly accelerates to its terminal speed of $1.0\,\mathrm{m\,s^{-1}}$ (Figure 7, right panel), attaining $0.75\,\mathrm{m\,s^{-1}}$ at a depth of 3 m. In quiescent waters, the fall-rate typically varies by less than 1 %. Much larger variations are evident in this profile and this is due to the vertical motions of the turbulent eddies in Islay Sound.

The vertical component of turbulent velocity is not the only component that buffets the profiler. The vertical shear of horizontal velocity will impart a torque (or lift-force) that perturbs the along-body axis of the profiler from its normally vertical orientation (Figure 7, left panel). The measurement is for one axis only, and is labelled “roll”. In quiescent waters the typical roll angle is less than 0.5°. In Islay Sound the roll angle is typically three times larger and reaches 3° below 50 m, when the profiler is less than 15 m above the bottom.

A depth-independent horizontal flow has no effect on the orientation of the profiler because it merely translates it horizontal, and the instrument behaves as if the horizontal velocity were zero. The vertical profile of the roll angle is structurally similar to that of the fall-rate for two reasons – vertical turbulent velocity is generated by the horizontal component of eddies and – there must be vertical shear over the span of a horizontally oriented eddy. However, it is not possible to use the roll angle to quantify the vertical shear because that would require a very accurate model of the dynamic behaviour of the profiler. It is a qualitative indicator of shear – large roll indicates large vertical shear for scales larger than a body length. Smaller scales have little effect on the roll angle because they average to zero over the length of the

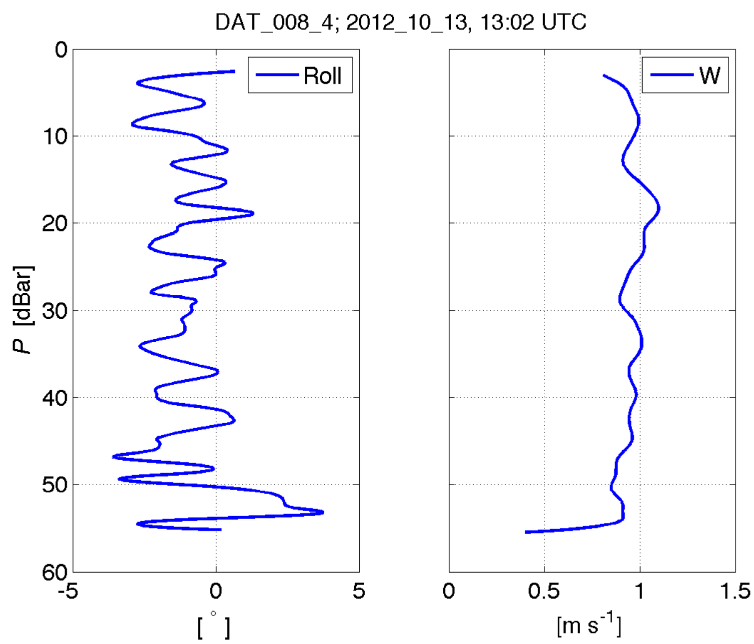

Figure 7: The deviation of the axis of the profiler, or its roll angle in degrees – left panel. The vertical velocity of the profiler, in $\mathrm{m\,s^{-1}}$ – right panel. The vertical axis is the pressure in units of dBar, which is numerically almost identical to depth in metres.

profiler.

5.2 Vibration

The shear probe, like all velocimeters, is a relative velocity sensor – it measures the vector difference of the water velocity and the profiler velocity. This makes the shear probe sensitive to vibrations of the profiler. The two horizontal components of the vibration are measured with two accelerometers for frequencies larger than 0.1 Hz (Figure 8).

The vibrational contamination can be removed with the "coherent noise removal" technique described by Goodman, et al [14]. The vibration data shown here are not converted into physical units because the Goodman technique requires only a signal that is linear with respect to acceleration. The data are left in terms of raw output, [counts], from the analog-to-digital converter. In addition, we do not record the vibrational acceleration, rather, we record its rate-of-change, for well-founded technical reasons that improve the signal-to-noise ratio [15]. Time differentiation boosts a signal proportion to its frequency, and this gives the profile a high-kurtosis appearance.

In Islay Sound, the vibrations are only a few times larger than in open-ocean profiles but the shear probe signals are larger by several factors of 10. Consequently, no correction for vibrations is required for any frequency larger than about 5 Hz. This is demonstrated explicitly in the presentation of spectra (section 5.6). The instrument vibrates more strongly in the x- than in the y-direction (the red and blue traces in Figure 8, respectively), and this

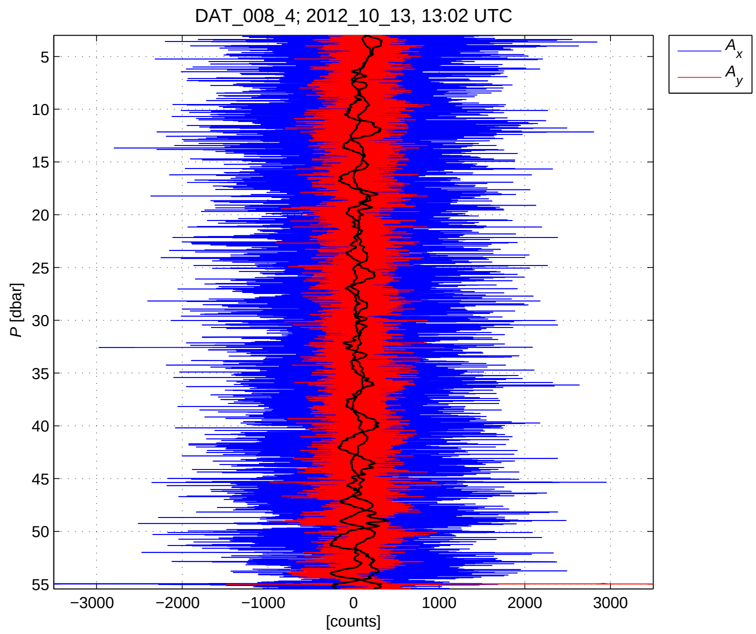

Figure 8: The rate-of-change of horizontal acceleration along the nominally horizontal x- and y-directions of the profiler – blue and red traces, respectively. The black traces are the same signals low-pass filtered at 1 Hz. The data are not converted into physical units.

is due to the differing stiffness of the internal frame in these two directions. However, the low-frequency vibrations (thin black lines in Figure 8) are comperable.

5.3 Temperature

The profile of temperature measured by the two fast thermistors is rich in vertical structure (Figure 9). The background temperature gradient is stably stratified, but it is punctuated by numerous temperature inversion, mainly due to the horizontal eddies sweeping deeper water upwards while also pushing shallower water downwards. Quantitative insight into the scales of these eddy motions is provided by the vertical scale of the temperature reversals. For example, the water in the depth range of 9 to 22 m "belongs" to the depth range of 24 to 38 m, and visa versa. The vertical displacement of water parcels by the eddy motions can be formally quantified by calculating the Thorpe scale [16], whereby the temperature profiles is resorted into a monotonic profile and noting the distance that each measured point has to be moved vertically in order to achieve this monotonicity. We have not yet calculated the Thorpe scale, but visual inspection of the temperature profile indicates that the typical vertical displacement is $O(10\,\mathrm{m})$ for the depth range of 10 to 40 m and that there are numerous smaller-scale displacements at other positions, such as the approximately 5 m scale inversions at 42 and 52 m depths.

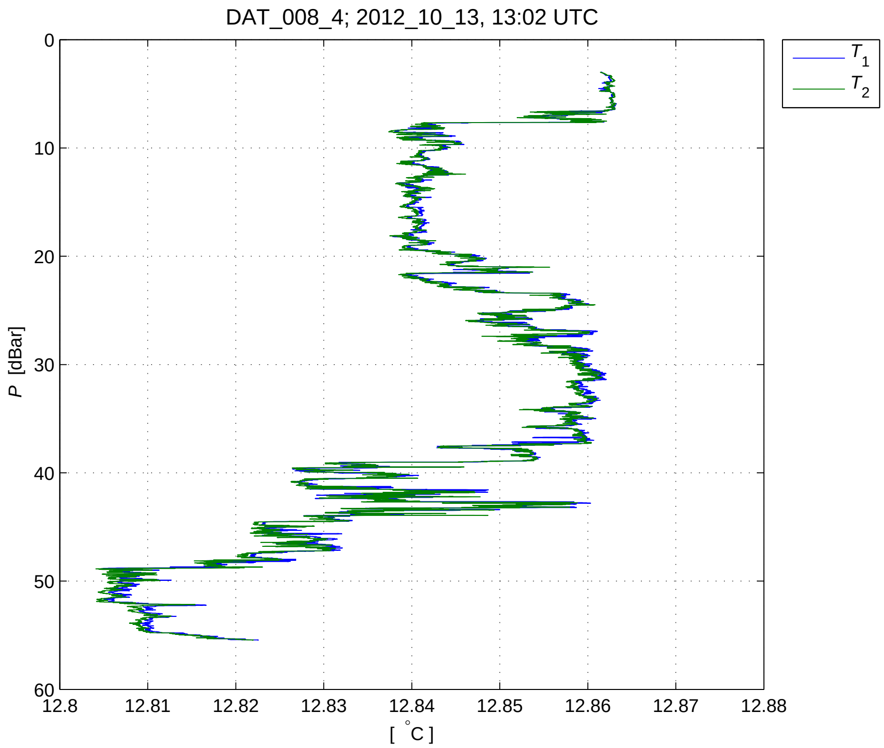

Figure 9: The vertical profile of temperature from the two thermistors, T_1 (blue) and T_2 (green).

5.4 Shear and Vertical Temperature Gradients

The vertical profile of the vertical gradient of horizontal velocity (usually labeled sh_1, or $\partial u_1/\partial z$ and the orthogonal component (usually labeled sh_2, or $\partial u_2/\partial z$) are shown in Figure 10. The variance of shear is dominated by the short length-scale components and is not uniformly distributed with respect to depth. Intermittency is almost a defining characteristic of turbulence. The shear variance is largest in the bottom 7 metres of the profile (within 17 m of the bottom), and this elevation of the turbulence is very likely due to bottom drag. However, the variance above this layer is nearly as large as in the lowest layer. The variance is much reduced for a short region near 48 m and this corresponds very precisely with the sharp drop in temperature at the same depth (Figure 9). That is, this local minimum of shear variance is located at the edge of an overturning eddy.

The eddy edge (Figure 11 and 12) is only 0.4 m and wide and spans from 47.5 to 47.9 m. The large values of shear and vertical gradients of temperature are mainly due to small-scale $O(0.01\,\text{m})$ variations.

The shear can be integrated vertically to deduce the vertical profile of horizontal velocity fluctuations, u' v', which we denote by u_1 u_2, because we do not know the actual geographic orientation of the probes, other than that the two components are orthogonal. This integral will not provide velocity variations that have scales bigger than about one profiler length because, for the larger scales, the profiler will move horizontally with the local water and report zero *relative* velocity. The instrument inherently acts to high-pass filter its measurements.

In addition, the shear probe signal itself is high-pass filtered (at 0.1 Hz) by the electronics and is high-passed again (at 0.25 Hz) by post-cruise data processing. The velocity profiles are shown in section 5.8.

The shear is used to estimate the rate of dissipation of TKE (Turbulence Kinetic Energy) because that rate is proportional to the variance of shear (16). This is a fundamental parameter that characterizes the intensity of turbulence and gives the rate at which energy flows from the largest scales to the smallest scales, where it is irreversibly converted to heat by molecular friction. The variance of shear is best estimated in wavenumber space, so spectra are presented next, before we present the dissipation rates.

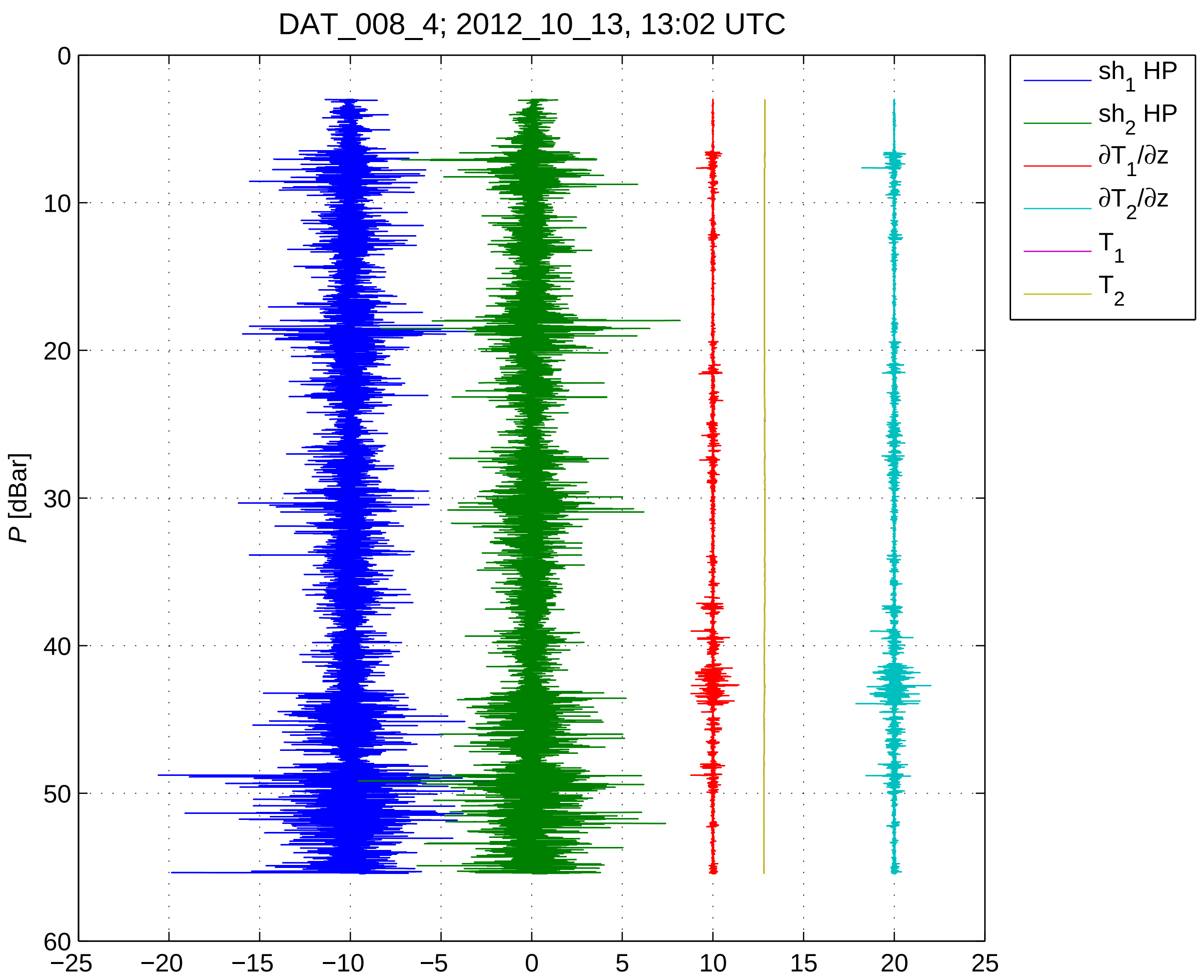

Figure 10: The vertical profiles of the vertical shear from probe 1 (sh_1, or $\partial u_1/\partial z$) – blue – and probe 2 (sh_2, or $\partial u_2/\partial z$) – green; the vertical gradients of temperature from probe 1 ($\partial T_1/\partial z$) – red – and probe 2 ($\partial T_2/\partial z$) – cyan –; and their temperatures, T_1 and T_2 – magenta and gold, respectively. (NB: T_1 and T_2 are identical, so their lines are identical). The vertical gradients all have a mean of nearly zero, and have been intentionally offset by -10, 0, 10 and 20 units for clarity.

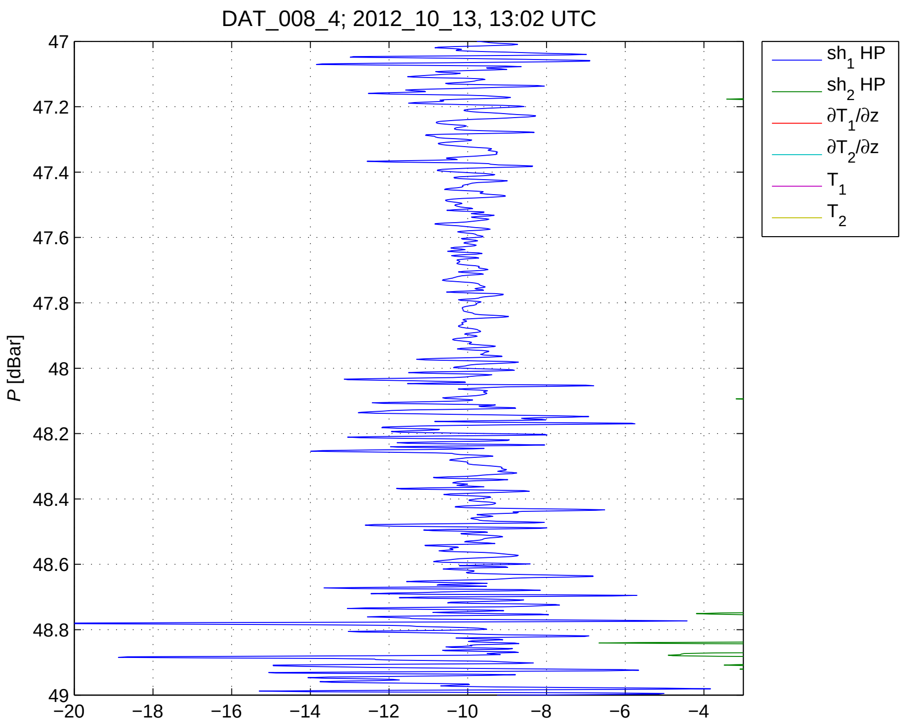

Figure 11: A close up view of $\partial u_1/\partial z$ for the depth range of 47 to 49 m.

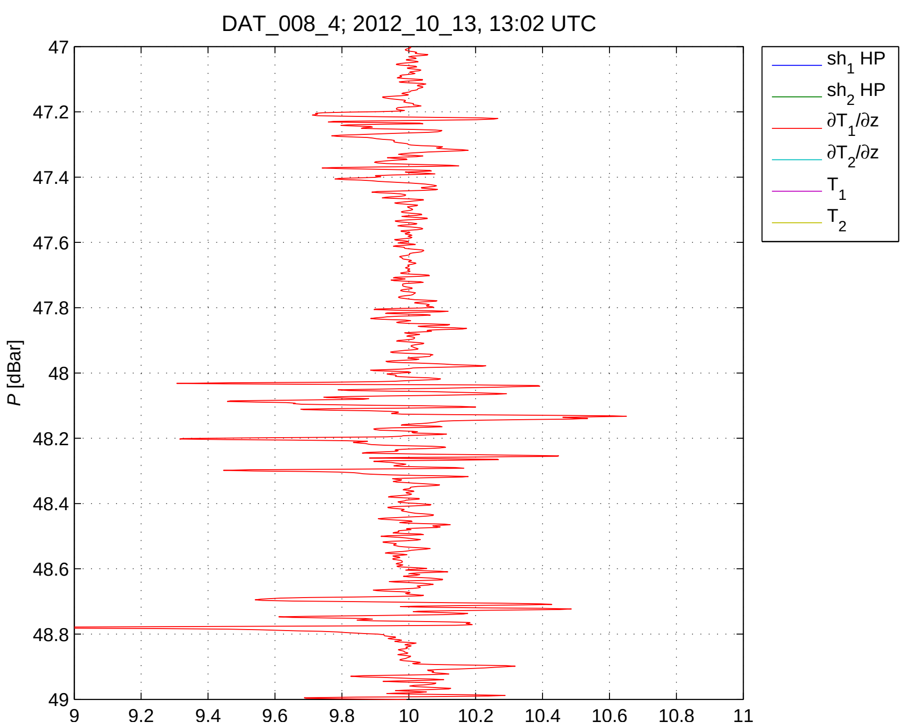

Figure 12: A close up view of $\partial T_1/\partial z$ for the depth range of 47 to 49 m.

5.5 Frequency Spectra

Frequency spectra of horizontal vibrations, vertical shear, and the gradient of temperature are shown in Figure 13, for the depth range of 20 to 30 m. We follow the convention that the variance of some signal, say η, equals the integral of its spectrum, ϕ,

$$\overline{\eta^2} = \int_0^{f_N} \phi(f)\mathrm{d}f \tag{11}$$

where f_N is the Nyquist frequency, which equals one-half of the sampling rate, and the over-line represents an average. Likewise,

$$\int_{f_1}^{f_2} \phi(f)\mathrm{d}f \tag{12}$$

gives the variance of η for the frequency band of f_1 to f_2, where $f_2 > f_1$.

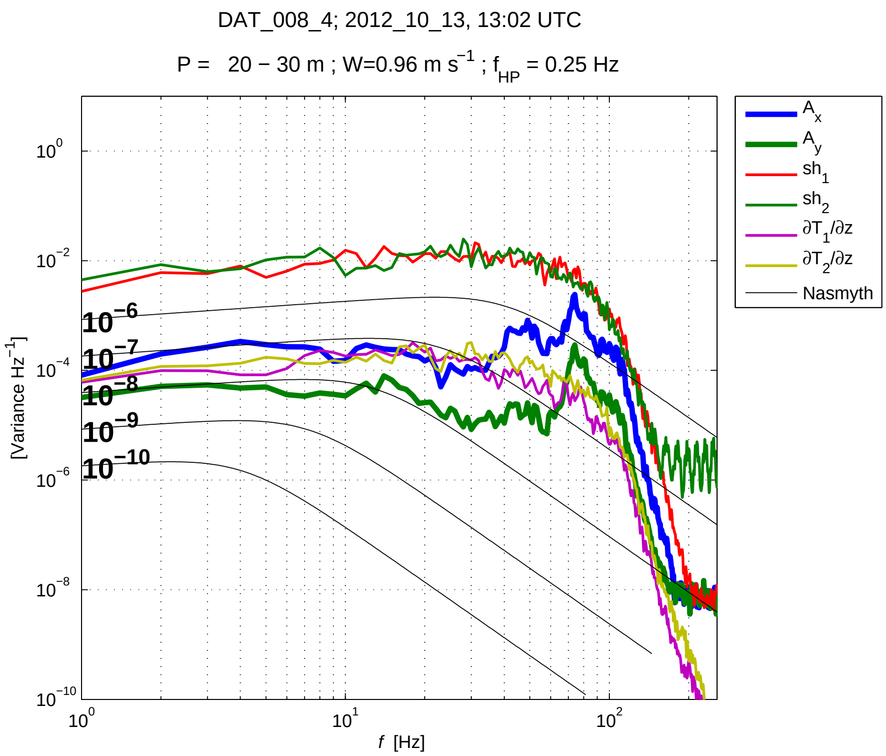

Figure 13: Frequency spectra of horizontal acceleration, shear, and the vertical gradient of temperature for the depth range of 20 to 30 m. These spectra are identified by colour and line thickness in the legend (upper right corner). The thin black lines are the empirical Nasmyth spectra for dissipation rates of 1×10^{-10} to 1×10^{-6} W kg^{-1}. The acceleration spectra have been shifted to bring them to a level comparable to the shear spectra.

All spectra fall off steeply above 100 Hz because of the anti-aliasing filters in the profiler. The vibration spectra (thick lines) have peaks near 45 and 75 Hz which are known intrinsic features of the VMP-200 profiler. Also, vibrations are stronger in the x- than in the y-direction (which was noted in Figure 8), and this is due to the structure of the internal frame that holds the electronics. It is much stiffer in the y-direction than in the x-direction. The spectral peaks of vibration do not have any signature in the shear spectra (thin red and green lines) which indicates that the environmental signal is much larger than the vibrations. In other words, the horizontal velocity of the profiler, due to vibrations, is insignificant compared to the velocity of the water, at least for frequencies higher than 40 Hz.

The temperature gradient spectra roll off near 30 Hz, corresponding to the frequency response of the FP07 thermistor (section 2.5) while moving a speed of $1\,\mathrm{m\,s^{-1}}$. This means that features with vertical wavelength smaller than ≈ 0.03 m are attenuated. Temperature fluctuations with the very smallest scales, such as the thin gradients in Figure 12, may be larger than shown.

The thin black lines in Figure 13 are the Nasmyth empirical wavenumber spectra converted into frequency spectra for five different levels of the rate of dissipation of TKE. They are explained in the next section.

5.6 Wavenumber Spectra

The frequency spectra are converted into wavenumber spectra using the "Taylor Frozen Field Hypothesis" (7, 8). The wavenumber spectrum, $\psi(k)$, derived from a frequency spectrum, $\phi(f)$, must still represent variance, according to our definition in (11). Consequently,

$$\psi(k)\ \mathrm{d}k = \phi(f)\ \mathrm{d}f = W\phi(f)\ \mathrm{d}\,(f/W) \tag{13}$$

where

$$k = f/W \tag{14}$$

is the wavenumber in cycles per metre (cpm) and satisfies (8). Thus, the wavenumber spectrum is related to the frequency spectrum by

$$\psi(k) \ = \ W\phi(f)\ . \tag{15}$$

The wavenumber spectra of shear are shown by the red and green lines in Figure 14. The spectra have been corrected for the spatial averaging of the probes using (10). The thin red and green lines are the spectra of shear without any correction for the vibration of the profiler, whereas the thick lines are the spectra after correction using the Goodman coherent noise removal algorithm. The difference between the noise-corrected and the uncorrected spectra is only significant for wavenumbers smaller than ≈ 4 cpm. That is, eddies with vertical wavelengths larger than ≈ 0.25 m buffet the profiler by a small, but detectable, amount.

The solid and dashed black lines in Figure 14 are the Nasmyth empirical spectra for turbulence with a dissipation rate of 6.9×10^{-6} and $7.0 \times 10^{-6}\,\mathrm{W\,kg^{-1}}$, respectively. The measurements of Nasmyth [17, 18, 19] provide the spectral level and shape of shear in high Reynolds

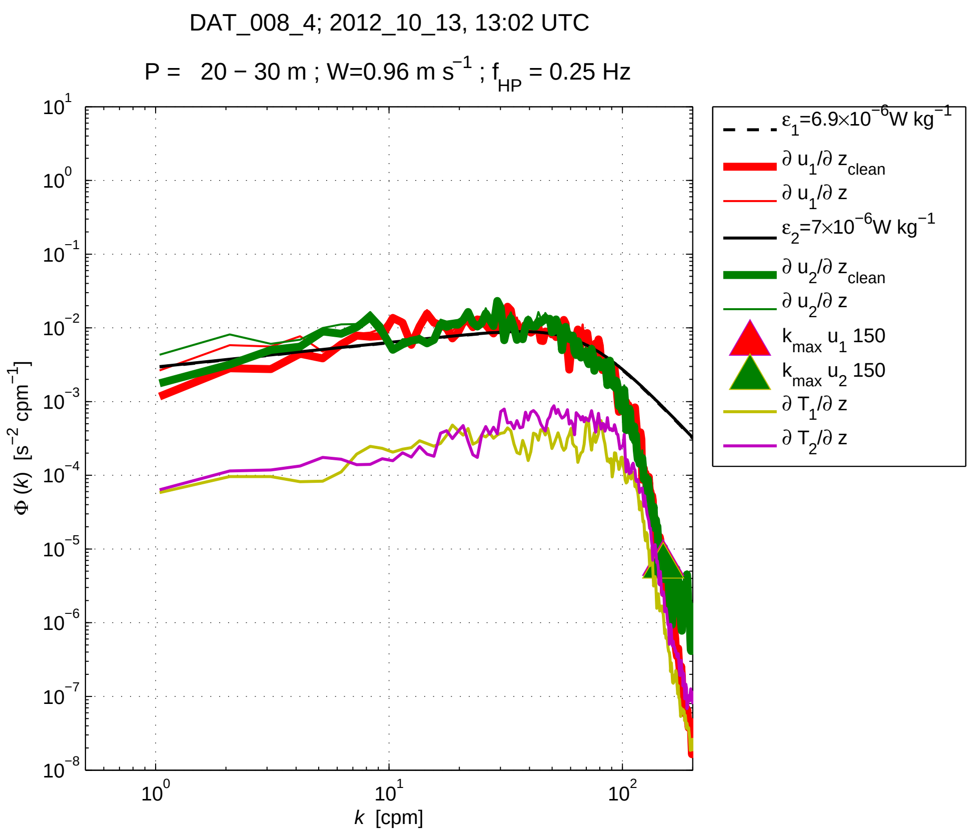

Figure 14: Wavenumber spectra of shear (red and green) and the vertical gradient of temperature (magenta and gold) for the depth range of 20 to 30 m. The thin red and green lines are the spectra without coherent-noise correction and the thick lines are the spectra after correction. The solid and dashed black lines are the empirical Nasmyth spectra for the dissipation rates indicated in the legend (upper right corner). The dashed line is almost completely covered by the solid line.

number turbulence. The high-wavenumber roll-off due to viscosity was not predicted by the classic Kolmogrov theory [20]. The Nasmyth spectrum represent the canonical expectation for a shear spectrum, and is used to judge of a shear measurement. The shear spectrum rises with a slope of 1/3 (because the velocity spectrum is proportional to $-5/3$), at low wavenumbers (the inertial subrange) and rolls-off at high wavenumbers (due to molecular viscosity).

The rate of dissipation of TKE is proportional to the area under the shear spectrum because, for isotropic turbulence,

$$\epsilon_1 = \frac{15}{2}\nu\overline{\left(\frac{\partial u_1}{\partial z}\right)^2} = \frac{15}{2}\nu\int_0^\infty \psi(k)\, \mathrm{d}k \tag{16}$$

where ν is the kinematic viscosity of seawater ($\approx 1 \times 10^{-6}\,\mathrm{m^2\,s^{-1}}$). A second and statistically independent estimate is provide by the second shear probe. It is not always possible to capture all variance of velocity shear. When the rate of dissipation is very small – which is not a problem for measurements in tidal channels – the higher wavenumbers may have contamination from vibrational and electronic noise, and the upper limit of integration is trimmed to a value that excludes the noise portion of a spectrum without also excluding significant variance from environmental shear. For very large dissipation rates – which are characteristic of tidal channels – the highest wavenumbers of shear are attenuated by the anti-aliasing filters that are required for faithful data sampling. For the measurements reported here, the anti-aliasing filters were set to 100 Hz $\approx$ 100 cpm, and they attenuate the spectrum for higher wavenumbers. The measured spectrum is definitely below the Nasmyth spectrum for $k > 100$ cpm. An easily applied correction accounts for the limited bandwidth of the measurements, and for this example the correction is fairly small. The correction is proportional to $\epsilon^{1/4}$ and becomes significant when the rate of dissipation is extremely large. The coloured triangles in Figure 14 indicate the limit of integration used to make the initial estimate of the rate of dissipation of TKE.

The wavenumber spectra of the vertical gradient of temperature are the thin gold and magenta lines in Figure 14. They have been corrected for the limited frequency response ($\approx$ 30 Hz) of the thermistor using the highest reported cutt-off frequency, which also applies the least amount of correction. The temperature gradient spectra rise with an initial slope of $+1/3$ and steepen to a slope of $+1$ at higher wavenumbers according to the theoretical predictions of Batchelor [21]. The high-wavenumber roll-off due to molecular diffusion is well above the anti-aliasing frequency and is not resolved.

The most intesne turbulence in this profile is near the bottom in the depth range of 48–55 m which is 9–17 m above the bottom. The rate of dissipation of TKE is 6.6×10^{-5} and $5.3 \times 10^{-5}\,\mathrm{W\,kg^{-1}}$ from shear probes 1 and 2, respectively (Figure 15).

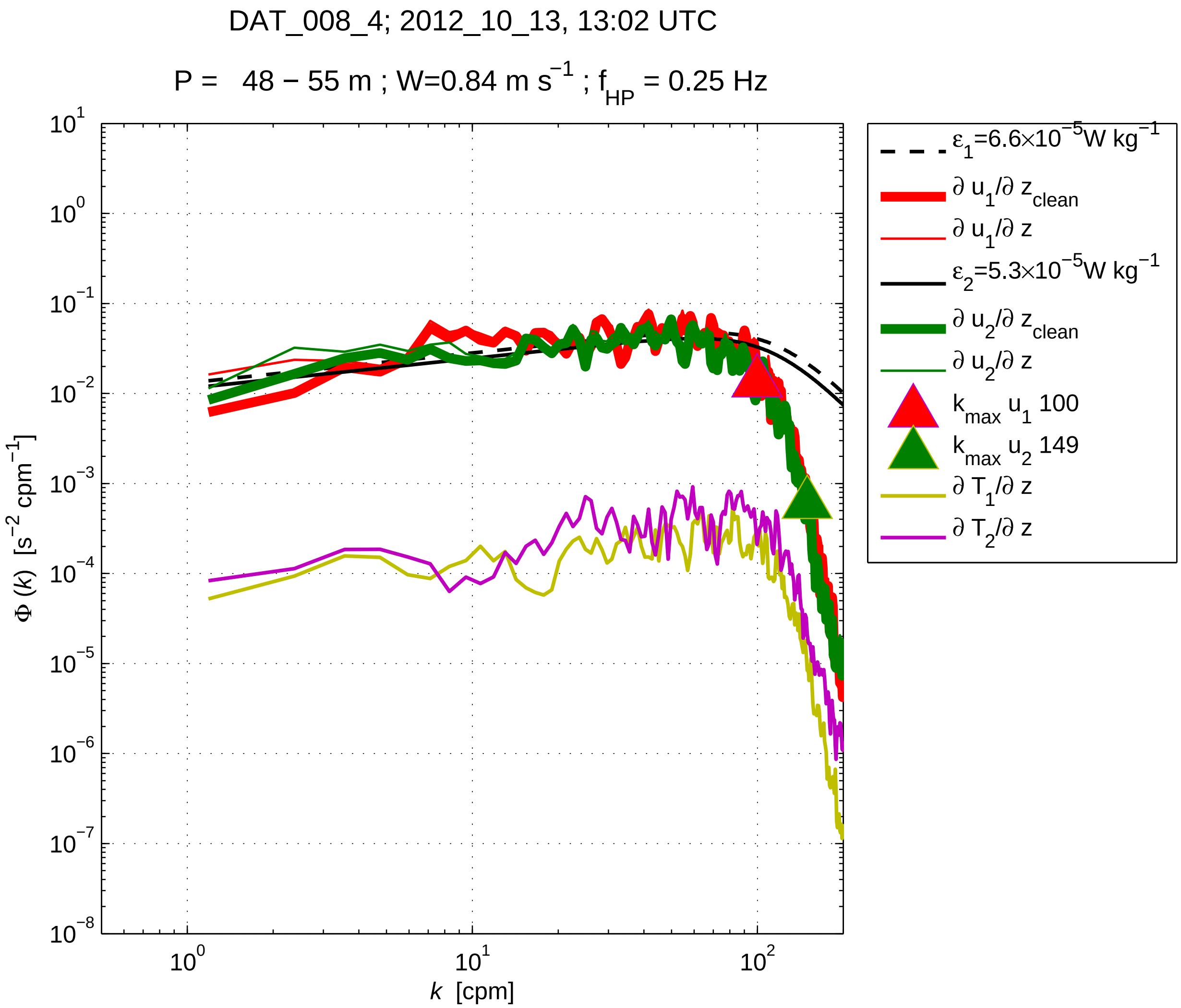

Figure 15: Wavenumber spectra from the depth range of 48–55 m. The line identification is the same as in Figure 14.

5.7 Dissipation Rate Profile

The rate of dissipation has been calculated for depth bins of approximately 3 m with 50 % overlap for the entire profile (Figure 16) and show that this rate can vary by several factors of 10 in the water column. The vertical distribution of turbulence is neither homogeneous, nor does it decrease monotonically with increasing height above the bottom. In tidal channels the shear is strong, which makes its bandwidth wide, and this allows for even finer depth resolutions of the rate of dissipations. Depth bins as small as 1 m are possible, should that be of value.

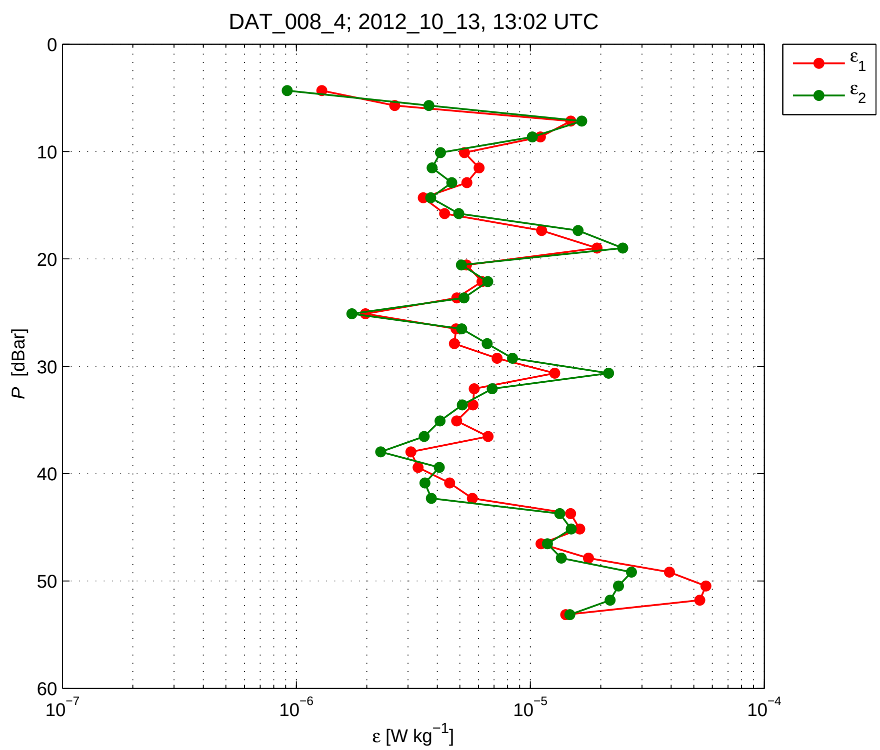

Figure 16: Vertical profile of the rate of dissipation of TKE, ϵ, for shear probe 1 (red) and 2 (green), estimated over depth bins of approximately 3 m with 50 % overlap.

5.8 Velocity Profiles

The vertical shear of horizontal velocity fluctuations (as shown in Figure 10) can be integrated vertically to produce full-depth profiles of turbulent horizontal velocity fluctuations (Figure 17), with the caveat that the largest vertical scales are not resolved by the shear probes mounted on a vertical profiler. The integrations have been applied to wavelengths shorter than 4 m. Larger-scale features are not resolved. Peak velocities are 0.08 m s^{-1} over most of the profile and reach 0.2 m s^{-1} in the bottom layer. The root-mean-square (rms) of a velocity component is typically three times smaller than its peak value. The total rms-velocity q, given in (5), is $\sqrt{3}$ times larger than an individual velocity component, if the turbulence is isotropic – a highly likely condition in a weakly stratifies tidal channel. The vertical velocity component, u_3 is not measured by the profiler. The total rms-velocity is thus 0.05 m and instantaneous peak values are 0.15 m. In the bottom layer all of these values are larger by a factor of 3.

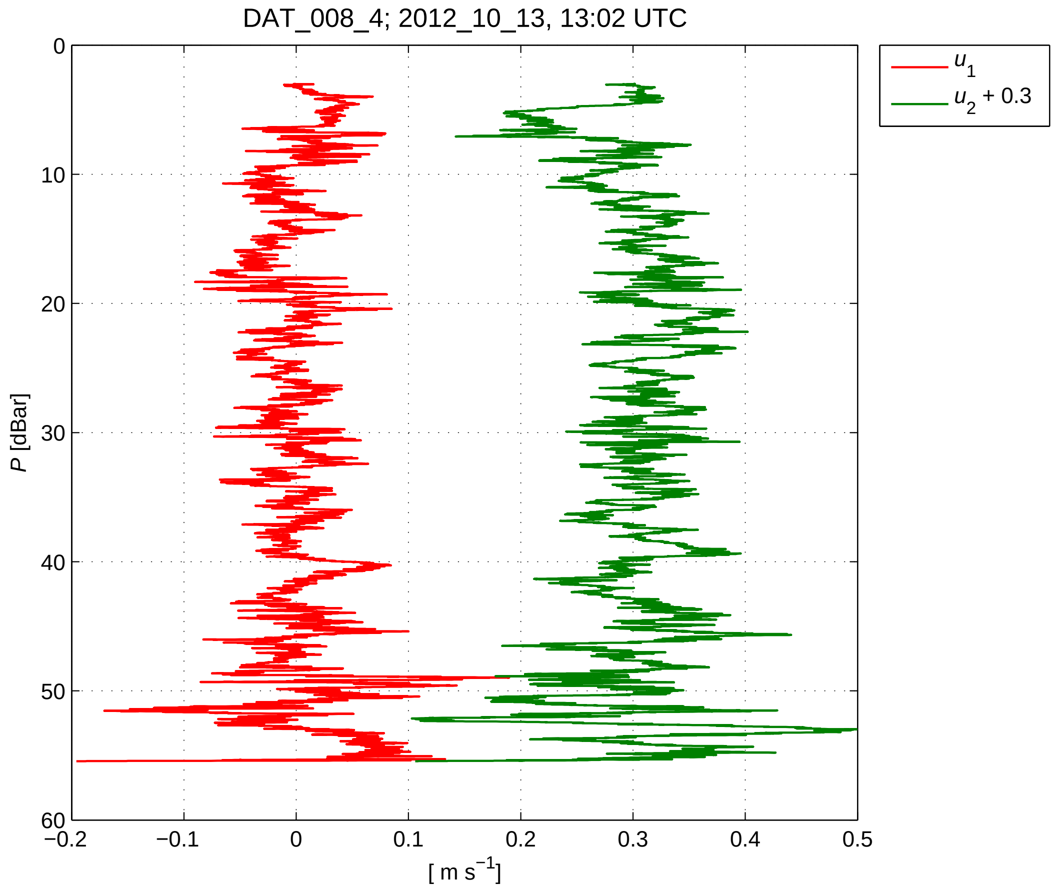

Figure 17: The horizontal turbulent velocity fluctuations from shear probe 1, u_1 (red), and the orthogonal component from shear probe 2, u_2 (green), derived by integrating the vertical shear. The velocity component u_2 has been intentionally offset, by the amount indicated in the legend, for clarity.

The local structure of the turbulent velocity fluctuations is visible in a section from depth 50–52 m (Figure 18). Eddies are imbedded within eddies and significant velocity changes can occur over a distance of only 0.04 m, such as the feature near the depth of 51.35 m, where the u_1 component shifts from -0.12 to 0.02 and back to 0.15 m s^{-1} over an interval of only 0.06 m.

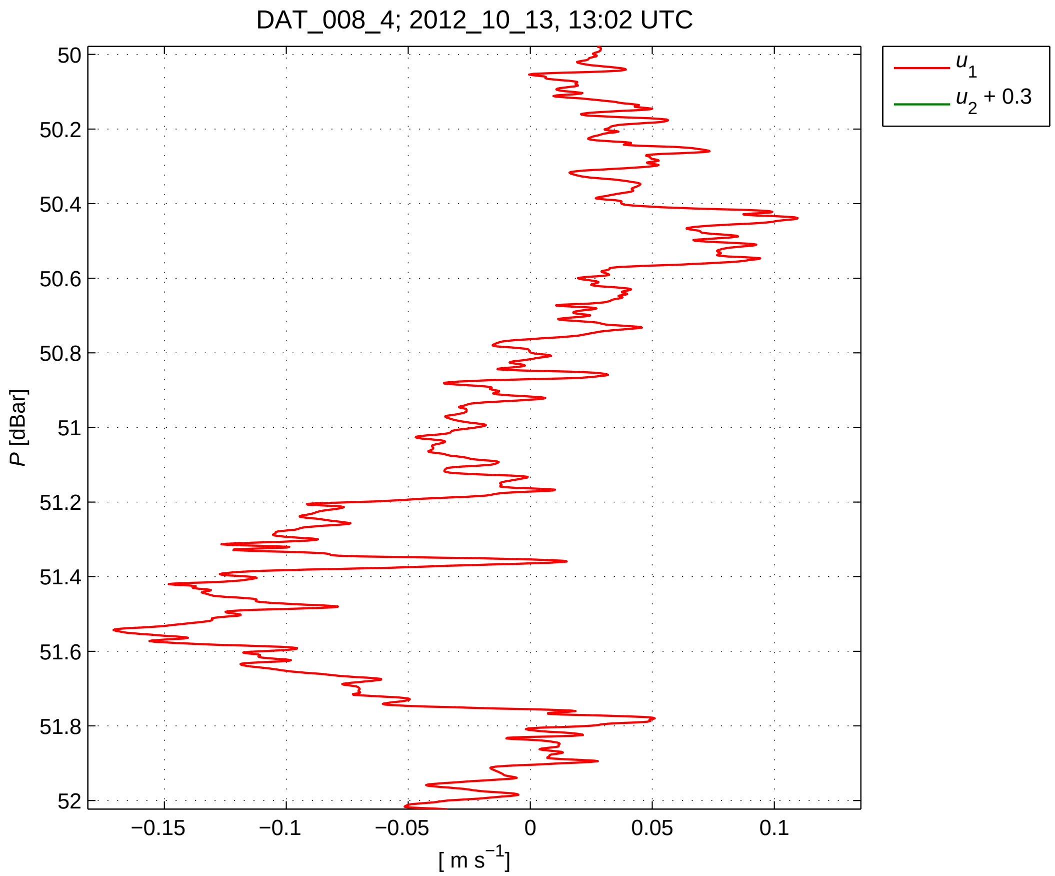

Figure 18: The horizontal turbulent velocity fluctuations from shear probe 1, u_1 (red), and the orthogonal component from shear probe 2, u_2 (green), derived by integrating the vertical shear. The velocity component u_2 has been intentionally offset, by the amount indicated in the legend, for clarity.

6 Corryvreckan Sound

An example of where the VMP-200 profiler is driven slightly beyond its limits (as configured for this work) is found in profile 013-9, which was collected in Corryvreckan Sound (Figure 19) when the flood was running seawater at nearly $4\,\mathrm{m\,s^{-1}}$.

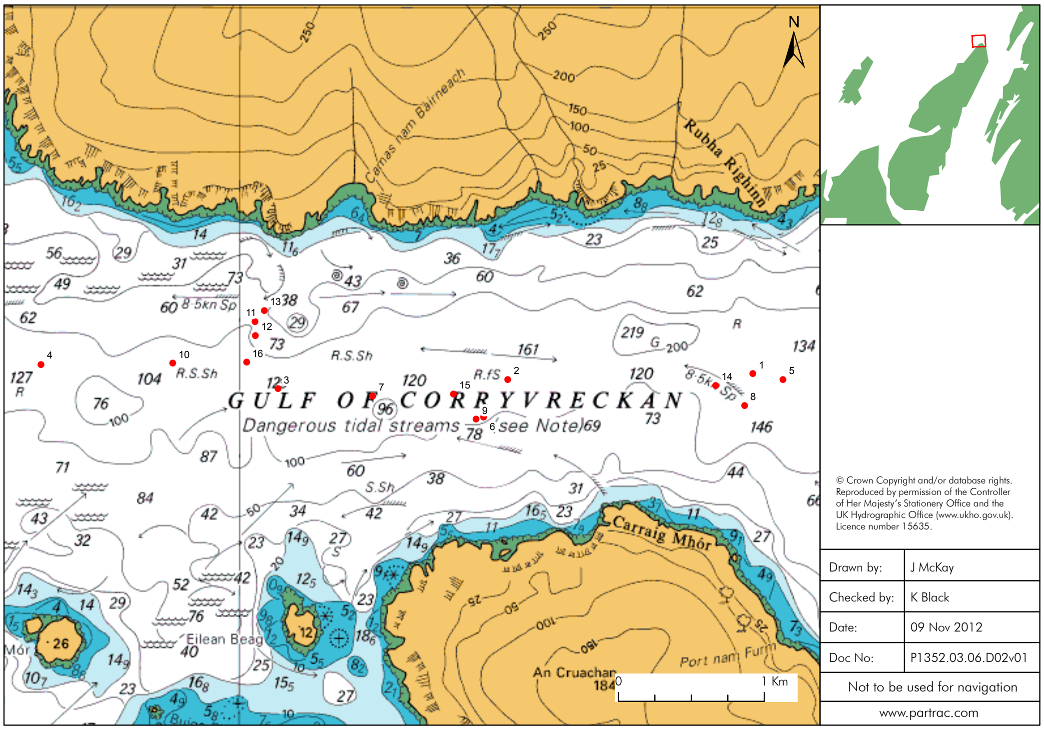

Figure 19: The location (red dots) of the VMP-profiles take in Corryvreckan Sound on 2012-10-12 and -14.

The roll of the profiler (Figure 20) is about twice as strong as in the previous example (Figure 7) and a single very strong event caused the profiler to roll by 15° at a depth of 65 m. The rate-of-change of pressure is consistently larger than the equivalent of $1.0\,\mathrm{m\,s^{-1}}$ while the profiler is shallower than 45 m, and it is consistently smaller than this nominal rate while it is deeper than 55 m. The profiler is experiencing a consistent down-draft of approximately of $0.25\,\mathrm{m\,s^{-1}}$ in the first half of its descent and an up-draft of similar strength, in the second half of its descent. This behaviour is easy explained by a pair of vortices, with one on top of the other.

On average, the temperature increases with depth (Figure 21), but the increase is only 0.017 °C from top to bottom. An abrupt jump occurs at 54 m and this location is precisely where the profiler rapidly slows from $0.8\,\mathrm{m\,s^{-1}}$ to $0.5\,\mathrm{m\,s^{-1}}$ (Figure 20). Large jumps in temperature also occur at 25 and 29 m depths. Inversions with short vertical scale occur throughout the water column.

The vertical profiles of shear (Figure 22) show an extremely intense feature between the depths of 52 and 68 m. This appears to be the top edge of the lower eddy. In this feature,

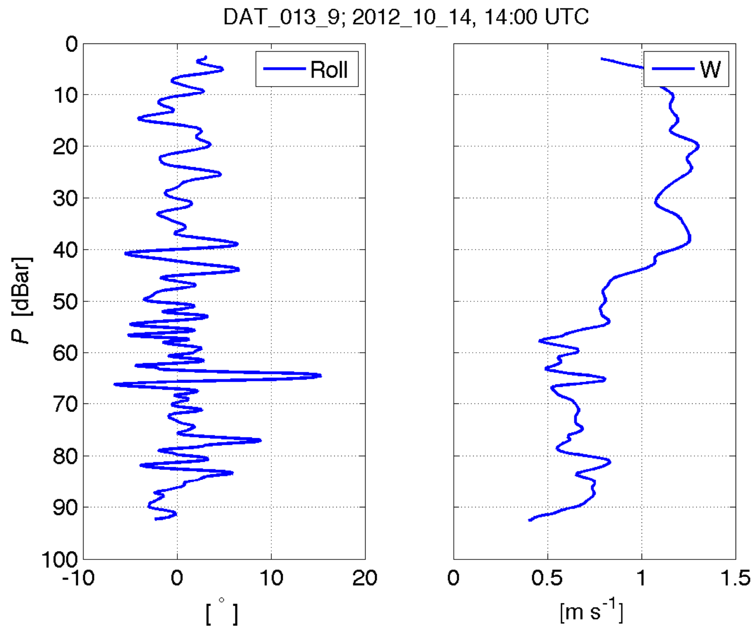

Figure 20: The roll-angle (left panel) and fall-rate (right panel) in Corryvreckan Sound.

peak shears reach $40\,\mathrm{m\,s^{-1}}$ per m.

The gradient of temperature is barely visible because the mean background gradient is only $190\,\mu^{\circ}\mathrm{C\,m^{-1}}$ and the horizontal graphing scale is large in order to accommodate the shear signals.

The spectrum of shear (Figure 23) for the turbulent feature between 52 and 68 m depth is extremely high, and the high-wavenumber roll-off, due to viscosity, is not resolved. The fit of the spectrum in the $+1/3$ range to the Nasmyth spectrum indicates that the rate of dissipation of TKE is $4.4 \times 10^{-3}\,\mathrm{W\,kg}$.

The vertical profile of the rate of dissipation of TKE (Figure 24), shows that the local maximum reaches $8 \times 10^{-3}\,\mathrm{W\,kg}$ at 64 m depth. This extremely large values of the rate of dissipation of TKE matches the largest rate ever measured in the ocean – in the Strait of Gibraltar – where the authors [22] also had to rely on fitting the Nasmyth spectrum to the $+1/3$ range of the spectrum. In Corryvreckan Sound, the range of the rate of dissipation of TKE is more than 1000:1.

The vertical profile of horizontal velocity (Figure 25) also reaches its extrema in the depth range of extreme dissipation rates. Peak values reach a magnitude of $1\,\mathrm{m\,s^{-1}}$ and, if true, indicate an angle-of-attack of 45°. This is well above the common (but unsubstantiated) notion that the AOA should be less than 20° and renders this measurement suspect.

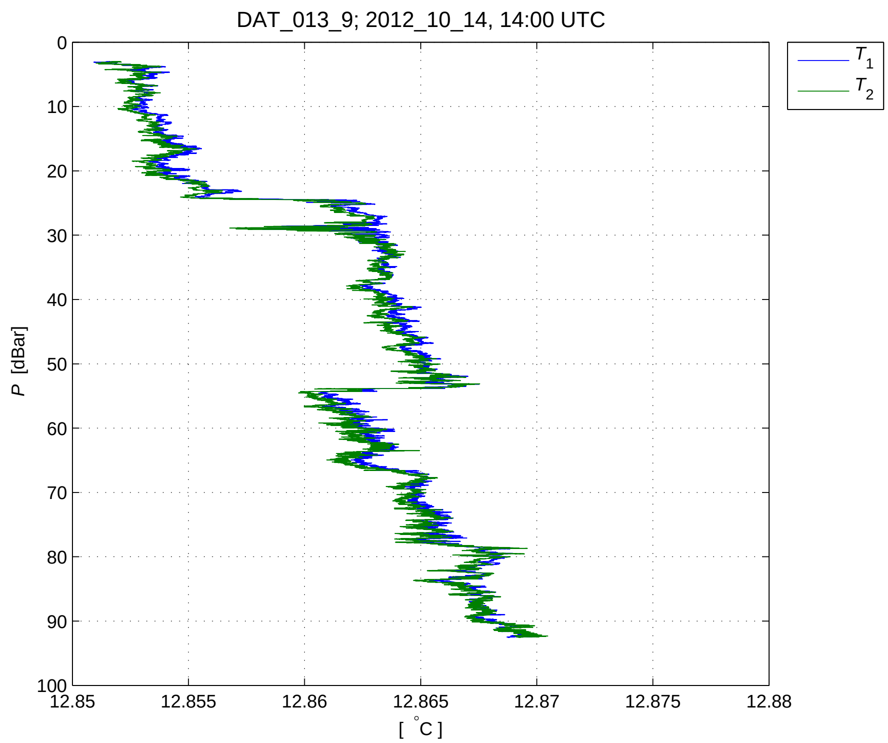

Figure 21: Vertical profile of temperature from the two thermistors.

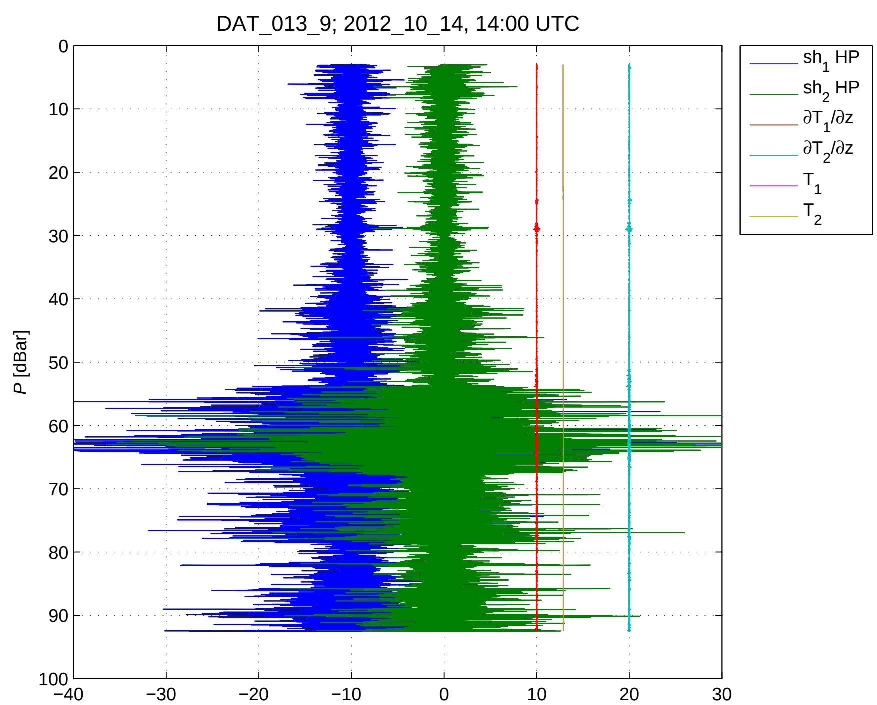

Figure 22: Vertical profile of shear, the vertical gradient of temperature, and temperature.

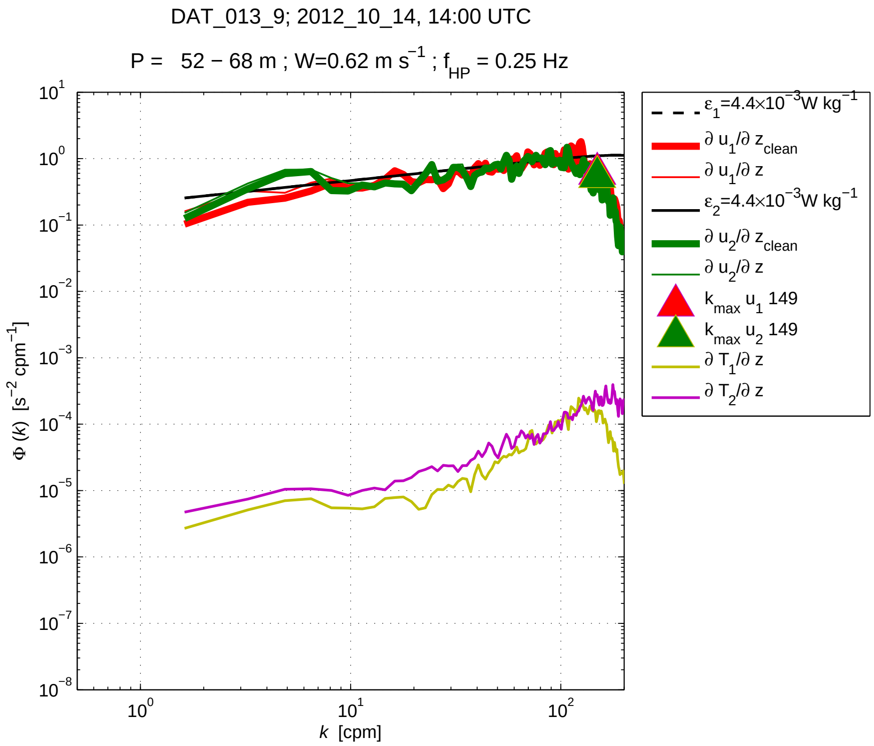

Figure 23: The wavenumber spectrum of shear (red and green lines, thick and thin) and the vertical gradient of temperature – magenta and gold.

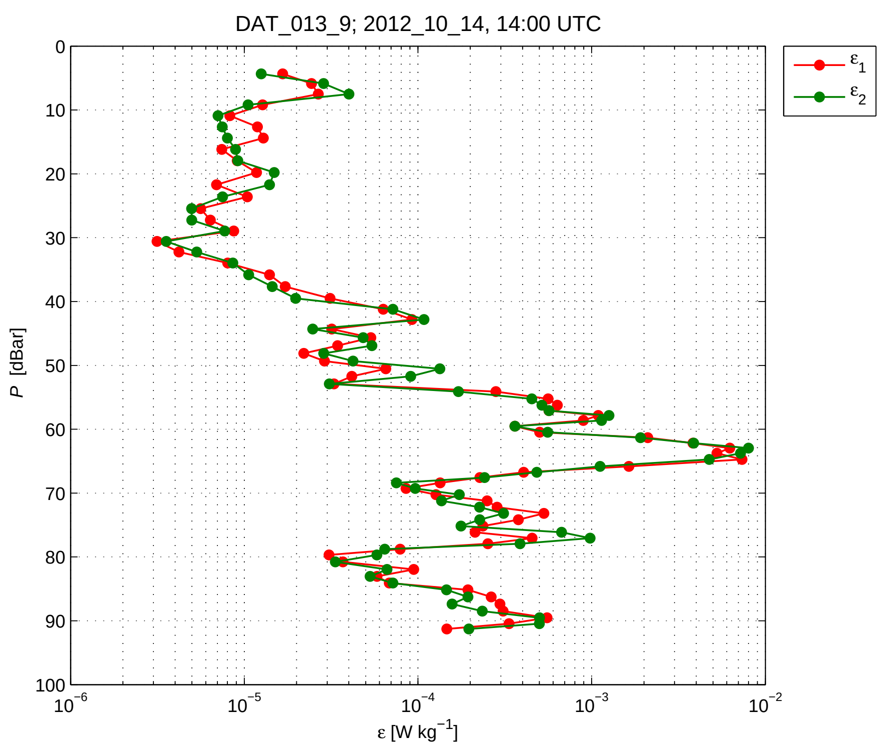

Figure 24: Vertical profile of the rate of dissipation of TKE, ϵ, for shear probe 1 (red) and 2 (green), estimated over depth bins of approximately 3 m with 50 % overlap.

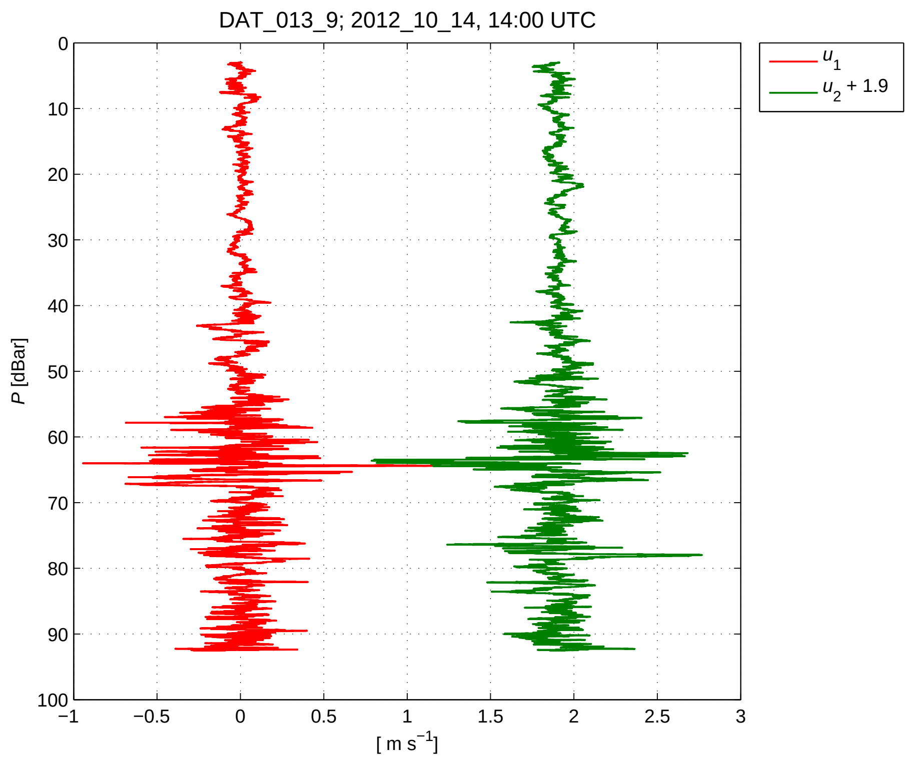

Figure 25: Vertical profile of the horizontal velocity derived from the shear probe data.

7 Comparison with Other Instrumentation

Although shear probes mounted on vertical profilers have been used for over 40 years for oceanic turbulence measurements, they are nearly unknown in the tidal energy community. Acoustic Doppler velocimeters (ADV) and acoustic Doppler current profilers (ADCP) are widely used, but they cannot provide a comprehensive measurement of the turbulence in the water column. In this section we provide a brief comparison of these three tools.

7.1 ADV

The ADV and the shear probe both are single point sensors, but there are some differences. An advantage of the ADV is that it provides a direct measurement of three orthogonal velocity components at a single point. It works from a stationary platform, while the shear probe has to move relative to the water. Also, the shear probe only measures two velocity components orthogonal to the mean flow direction. The spatial resolution of the shear probe (0.003 m), however, is five times smaller than the width of the sampling volume of the ADV, which is 0.015 m for the Nortek *Vector* ADV. The ADV requires particulates comparable in size to its acoustic wavelength (250 µm) in order to receive echoes from which it estimates the velocity. It does not work in clear water or in the presence of large amount of air bubbles. The shear probe does not require particulates.

The most significant difference between the shear probe and the ADV is noise. At 64 samples per second, the standard-deviation of ADV velocity noise is $0.02\,\mathrm{m\,s^{-1}}$, when this instrument is set to a full-scale range of $1\,\mathrm{m\,s^{-1}}$. (The noise is a fraction of the full-scale range.[2]) The peak-to-peak noise is six times larger. The environmental velocity features shown in Figure 17, if measured by an ADV, would have been obscured by noise, except for a small section in the bottom boundary layer where the signals are extremely strong. It is also not always possible to achieve the spatial resolution inferred by the ADV's sampling volume. When sampling at the typically maximum rate of 64 per second, the spacing of the samples is $W/64$ which is larger than the width of the sampling volume for $W > 1\,\mathrm{m\,s^{-1}}$. The spatial resolution of the shear probe is speed-independent.

7.2 ADCP

The ADCP is a remotely sensing velocity profiler and not a local point sensor. It has the potential to provide a time-series of vertical profiles, if certain conditions are satisfied. The time-mean profile of velocity is obtained if the environmental time-mean velocity is uniform over the horizontal distance spanned by the divergent acoustic beams of the ADCP. The homogeneity of mean velocity, over the beam spread, is usually satisfied in natural waters. Turbulence information can also be obtained if the turbulence is statistically homogeneous over the horizontal distance spanned by the beams. This condition is satisfied when topographic variations (such as bottom depth) are long compared to the spread of the beams. Large bottom obstacles near the ADCP will create statistical inhomogeneity that precludes the measurement of turbulence with the ADCP.

The beam-variance difference technique [23, 24, 25] has been used to derive the Reynolds stress and the turbulence kinetic energy in tidal channels where the bottom was relatively smooth. However, this technique is very sensitive to tilting of the ADCP and a 1° departure from level imparts an error of $10\,\%$ in the Reynolds stress. The vertical resolution is usually more than $4\,\mathrm{m}$.

7.3 Synopsis

The most outstanding difference between the shear probe and the other two instruments is in their spatial resolution and noise. In addition, the shear probe can be conveniently profiled to obtain in-situ profiles of the turbulent velocity fluctuations in the water column. Whereas the ADV and ADCP resolve scales of $O(\gtrsim 1\,\mathrm{m})$, the shear probe mounted on a vertical profiler resolves scales of $O(0.001 - 1\,\mathrm{m})$, with some possible overlap between the spatial resolution of the shear probe and the ADV around $O(1\,\mathrm{m})$ scales. The signal strength resolution, or equivalently the standard deviation of the measurement noise, is $O(0.001\,\mathrm{m\,s^{-1}})$ for the shear probe while it is $O(0.02\,\mathrm{m\,s^{-1}})$ for an ADV and even larger for an ADCP. The shear probe will provide information on the velocity field that is commensurate with the blade-width of turbines while the other two instruments provide the larger scale velocity field. Both

[2]Vector Current Meter User Manual, 2005, N300-100, Rev. H. NorteK AS

are important for understanding the forces that are exerted on underwater structures by the mean and turbulent flow in a tidal channel. In concert, these instruments can provide wide-scale, or broadband, spectral information.

8 VMP Optimization for Future Work

For the measurements presented here, the VMP-200 was configured exactly as it is for open-ocean work, where the range of the rate of dissipation of TKE is usually 1×10^{-11} to $1 \times 10^{-6}\,\mathrm{W\,kg^{-1}}$. For instance, dissipation rates in the surface mixing layer, when the winds are $\sim 20\,\mathrm{m\,s^{-1}}$ is $\sim 1 \times 10^{-7}\,\mathrm{W\,kg^{-1}}$. In tidal channels this is the bottom of the range. Therefore, the VMP-200 needs some adjustments for work in highly energetic tidal channels.

The gain of the electronics for the shear probes should be reduced by a factor of ~ 30. The signals saturated the electronics on two of the profiles taken on the lee side of the 30 m deep pinnacle in Corryvreckan Sound (Figure 19). This decrease is easily achieved. The VMP is typically trimmed for a fall-rate of $0.6\,\mathrm{m\,s^{-1}}$, but faster profiling is preferred for tidal channels for several reasons. The duration of a profile is reduced and this reduces the drift of the ship and the profiler. Eddy velocity is large in a tidal channel, and a fast fall-rate reduces the angle-of-attack. We trimmed the VMP to a fall-rate of $1.0\,\mathrm{m\,s^{-1}}$ for the work reported here, in anticipation of strong vortices. A further increase to approximately $1.5\,\mathrm{m\,s^{-1}}$ is desirable and achievable. Tests of higher fall-rates are in progress at the time of writing.

Faster profiling changes the requirements for sampling. The sampling rate and the anti-aliasing frequency must both be doubled. This, too, is easily achieved. The biggest operational challenge is the handling of the deployment line, which will become more difficult with increasing fall-rate. A winch system should be implemented, and preferably one that can eject the line into the water. RSI has such a winch, but it is large and may not be suitable for use on a small vessel with limited deck space, such as the one used for the work reported here.

With these improvements, it should be possible to take profiles to 60 m, recover the profiler, and reposition the ship for the next profile with a repeat time of 2 to 3 minutes.

9 Other Ways to Implement the Shear Probe

The shear probe has been mounted on other types of profilers, such as gliders, AUVs, submarines, towed vehicles, and moorings. The moored platform is not a “profiler” in the sense that some motive force propels it through the water. Here, the ambient current moves water over the shear probe, resulting in a time series of shear, $\partial w/\partial x$ or $\partial v/\partial x$, at a fixed point. A minimum speed is required – $\approx 0.05\,\mathrm{m\,s^{-1}}$ in order for the signal to exceed the electronic noise, and – a higher speed yet, in order for the angle-of-attack of the oncoming eddies to be within the range of the shear probe. The experimental challenge is to reduce the “draw-down” of the mooring by the drag force imparted by the very strong currents in a tidal channel. In addition, the mooring must be able to swivel so that it can point into the current on both phases of the tide, and the mooring harness must be gimballed so that it can maintain its horizontal orientation. Two such moorings (except for the gimbal) are currently in operation (Figure 26) – they carry shear probes, a Nortek Vector current meter, and motion sensors. If a rigid platform already exist, such as an in-place turbine, then the shear probe could be mounted on this structure to collect a time-series. At the moment, for the system shown in Figure 26, the size of non-volatile memory limits shear probe measurements to about 16 days of continuous operation. Longer time-series require intermittent sampling or the use of a shore cable.

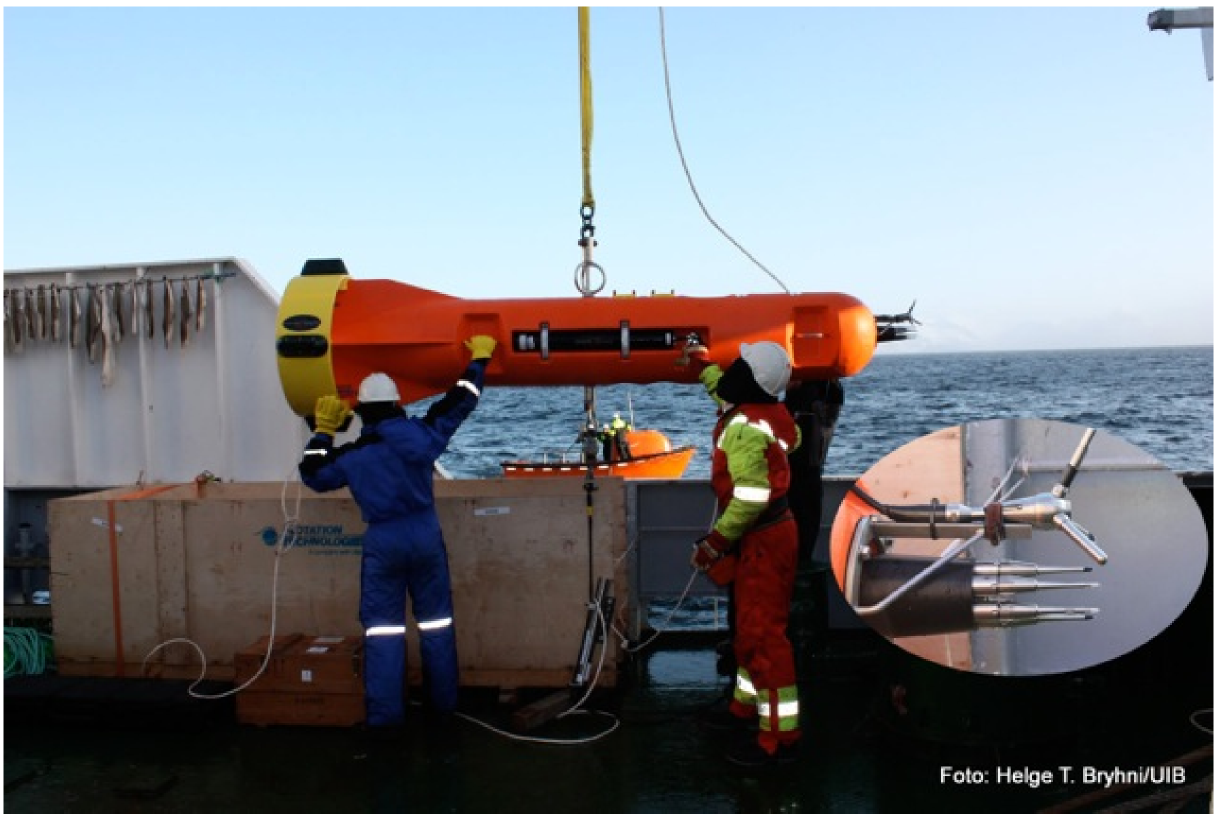

Figure 26: A turbulence measuring mooring being deployed. It carries shear probes, thermistors, and a Vector current meter (oval insert, lower right side). A nine-component motion package is inside of the pressure case. Photo courtesy of Helge Bryhni, University of Bergen.

10 Summary

The Vertical Microstructure Profiler, VMP-200, was used to obtain profiles of various turbulence parameters in two highly energetic tidal channels, Islay Sound and the Straight of Corryvreckan, which are locations for future commercial tidal energy generation. The VMP carried a set of shear probes and fast response thermistors. From the shear probe data, a variety of turbulence parameters were derived, such as profiles of turbulent kinetic energy dissipation, turbulence intensities, as well as velocity fluctuations on scales between approximately 0.01 to 1 m. The profiles of turbulent kinetic energy (TKE) dissipation exhibit a wide dynamic range of the turbulence, spanning several orders of magnitude from 1×10^{-6} to $\sim 10^{-2}$ W kg^{-1} in a single profile. Velocities derived from the shear probe measurements show strong fluctuations of the velocity, at times reaching rates of 0.14 m s^{-1} over 0.2 m depth range (equivalent to 3.5 m s^{-1} per m of depth).

The VMP profiler has also demonstrated its ease of deployment, providing full depth turbulence profiles of the channel without the requirement of large installations. When deployed in conjunction with other measurement technologies, such as ACDPs and ADVs, shear probe measurements can help overcome the limitations of scale resolution, time resolution, and measurement resolution in low energetic environments that are inherent in these instruments. The shear probe can complement acoustic technologies in tidal energy applications, thereby resolving a engineering unknowns.

Going forward, a dialogue with the tidal energy industry is necessary to identify the variables and parameters required by existing engineering models and adapt the data outputs provided by the VMP to these requirements. The ability to input a set of standardized site-specific turbulence measurements as inputs for device manufacturers and project developers could improve the technical and economic feasibility of tidal energy projects.

References

[1] H. Tennekes and J. L. Lumley. *A First Course in Turbulence*. MIT Press, 1989.

[2] P. K. Kundu. *Fluid Mechanics*. Academic Press, 1990.

[3] R. G. Lueck, F. Wolk, and H. Yamazaki. Oceanic velocity microstructure measurements in the 20th century. *Japan Journal of Oceanography*, 58:153–174, 2002.

[4] T. R. Osborn and C. S. Cox. Oceanic fine structure. *Geophysical Fluid Dynamics*, 3:321–345, 1972.

[5] T. R. Osborn and W. R. Crawford. An airfoil probe for measuring turbulent velocity fluctuations in water. In F. W. Dobson and R. Davis, editors, *Air-Sea Interaction: Instruments and Methods*, Mechanical Engineering, page 535. Plenum, 1980.

[6] P. Macoun and R. Lueck. Modelling the spatial response of the airfoil shear probe using different sized probes. *Journal of Atmospheric and Oceanic Technology*, 21:284–297, 2004.

[7] T. E. Siddon and H. S. Ribner. An aerofoil probe for measuring the transverse component of turbulence. *J. American Inst. Aeronautics and Astronautics*, 3:747–749, 1965.

[8] T. E. Siddon. A miniature turbulence gauge for utilizing aerodynamic lift. *Review of Scientific Instruments*, 42:653–656, 1971.

[9] T. R. Osborn. Local vertical profiling of velocity microstructure. *Journal of Physical Oceanography*, 4:109–115, 1974.

[10] H. Baumert, J. Simpson, and J. Suendermann. *Marine Turbulence: Theories, Observations and Models*. Cambridge University Press, 2005.

[11] M. C. Gregg and T. B. Meagher. The dynamic response of glass rod thermistors. *Journal of Geophysical Research*, 85:2779–2786, 1980.

[12] J. D. Nash, D. R. Caldwell, M. J. Zelman, and J. N. Moum. A thermocouple probe for high-speed temperature measurements in the ocean. *Journal of Atmospheric and Oceanic Technology*, 16:1474–1482, 1999.

[13] P. Vachon and R. G. Lueck. A small combined temperature-conductivity probe. In *Proceedings of the 1984 STD Conference and Workshop*, San Diego, California, USA, 1984.

[14] L. Goodman, E. R. Levine, and R. G. Lueck. On measuring the terms of the turbulent kinetic energy budget from an auv. *Journal of Atmospheric and Oceanic Technology*, 23:977–990, 2006.

[15] T. D. Mudge and R. G. Lueck. Digital signal processing to enhance oceanographic observations. *Journal of Atmospheric and Oceanic Technology*, 11:825–836, 1994.

[16] S. A. Thorpe. *An Introduction to Ocean Turbulence*. Cambridge University Press, 2007.

[17] P. W. Nasmyth. *Ocean Turbulence*. PhD thesis, University of Bristish Columbia, Vancouver, British Columbia, Canada, 1970.

[18] N. S. Oakey. Determination of the rate of dissipation of turbulent kinetic energy from simultaneous temperature and velocity shear microstructure measurements. *Journal of Physical Oceanography*, 12:256–271, 1982.

[19] F. Wolk, H. Yamazaki, L. Seuront, and R. G. Lueck. A new free-fall profiler for measuring bio-physical microstructure. *Journal of Atmospheric and Oceanic Technology*, 19:780–793, 2002.

[20] A. N. Kolmogorov. Local structure of turbulence in an incompressible fluid at very high reynolds number. *Doklady AN SSSR*, 4:299–303, 1941.

[21] G. K. Batchelor. Small-scale variations of convected quantities like temperature in a turbulent fluid. *Journal of Fluid Mechanics*, 5:113–139, 1959.

[22] J. C. Wesson and M. C. Gregg. Mixing at camarinal sill in the strait of gibraltar. *Journal of Geophysical Research*, 99:9847–9878, 1994.

[23] A. Lohrmann, B. Hackett, and L. P. Roed. High-resolution measurements of turbulence, velocity and stress using a pulse-to-pulse coherent sonar. *Journal of Atmospheric and Oceanic Technology*, 7:19–37, 1990.

[24] Y. Lu and R. G. Lueck. Using a broadband adcp in a tidal channel. part i: mean flow and shear. *Journal of Atmospheric and Oceanic Technology*, 16:1556–1567, 1999.

[25] Y. Lu and R. G. Lueck. Using a broadband adcp in a tidal channel. part i: turbulence. *Journal of Atmospheric and Oceanic Technology*, 16:1568–1590, 1999.

11 Appendix-A: List of profiles

Name	Profile	Range	Date	Time	P_max	Where	Lat	Lon	Depth	Speed
		in original data file		UTC	[dBar]		DD MM	DD MM	m	m/s
DAT_003	1	160 - 220	2012-10-12	13:46:00	27	Corryvreckan				
DAT_003	2	280 - 340	2012-10-12	13:48:00	27	Corryvreckan				
DAT_004	1	120 - 170	2012-10-12	14:18:54	35	Corryvreckan				
DAT_004	2	300 - 390	2012-10-12	14:21:54	54	Corryvreckan				
DAT_005	1	310 - 390	2012-10-12	15:02:44	61	Corryvreckan				
DAT_006	1	340 - 390	2012-10-12	16:11:06	65	Corryvreckan				
DAT_006	2	530 - 620	2012-10-12	16:14:16	74	Corryvreckan				
DAT_006	3	1410 - 1510	2012-10-12	16:28:57	74	Corryvreckan				
DAT_006	4	1620 - 1720	2012-10-12	16:32:26	60	Corryvreckan				
DAT_006	5	1900 - 2010	2012-10-12	16:37:07	72	Corryvreckan				
DAT_006	6	2960 - 3020	2012-10-12	16:54:46	50	Corryvreckan				
DAT_007	1	150 - 200	2012-10-13	10:48:11	31	Islay Sound				
DAT_007	2	340 - 380	2012-10-13	10:51:21	36	Islay Sound				
DAT_007	3	570 - 620	2012-10-13	10:55:11	31	Islay Sound				
DAT_007	4	1160 - 1210	2012-10-13	11:05:01	37	Islay Sound				
DAT_008	1	190 - 260	2012-10-13	12:11:51	56	Islay Sound				
DAT_008	2	470 - 530	2012-10-13	12:16:31	50	Islay Sound				
DAT_008	3	730 - 800	2012-10-13	12:20:51	46	Islay Sound				
DAT_008	4	3230 - 3300	2012-10-13	13:02:31	56	Islay Sound	55 50.373	06 05.822	56	
DAT_008	5	3520 - 3590	2012-10-13	13:07:21	52	Islay Sound				
DAT_008	6	3800 - 3880	2012-10-13	13:12:01	53	Islay Sound				
DAT_009	1	380 - 450	2012-10-13	14:06:03	54	Islay Sound				
DAT_009	2	940 - 1100	2012-10-13	14:15:23	46	Islay Sound				
DAT_009	3	1210 - 1270	2012-10-13	14:19:53	44	Islay Sound				
DAT_009	4	3270 - 3330	2012-10-13	14:54:13	49	Islay Sound				
DAT_009	5	3860 - 3920	2012-10-13	15:04:03	52	Islay Sound				
DAT_009	6	4175 - 4230	2012-10-13	15:09:18	50	Islay Sound				
DAT_009	7	6100 - 6150	2012-10-13	15:41:23	47	Islay Sound				
DAT_009	8	6600 - 6660	2012-10-13	15:49:43	49	Islay Sound				
DAT_009	9	6820 - 6880	2012-10-13	15:53:23	50	Islay Sound				
DAT_011	1	190 - 250	2012-10-13	18:00:52	47	Loch Crinan				
DAT_011	2	430 - 480	2012-10-13	18:04:52	41	Loch Crinan				
DAT_012	1	2000 - 2130	2012-10-14	9:38:17	109	Corryvreckan				
DAT_012	2	2760 - 2880	2012-10-14	9:50:57	100	Corryvreckan				
DAT_012	3	3290 - 3410	2012-10-14	9:59:47	94	Corryvreckan				
DAT_012	4	3770 - 3880	2012-10-14	10:07:47	103	Corryvreckan				
DAT_012	5	7090 - 7200	2012-10-14	11:03:07	107	Corryvreckan				
DAT_012	6	7830 - 7960	2012-10-14	11:15:27	102	Corryvreckan				
DAT_013	1	540 - 660	2012-10-14	12:05:44	102	Corryvreckan				
DAT_013	2	1610 - 1700	2012-10-14	12:23:34	65	Corryvreckan				
DAT_013	3	2540 - 2640	2012-10-14	12:39:04	59	Corryvreckan				
DAT_013	4	2890 - 2970	2012-10-14	12:44:54	76	Corryvreckan				
DAT_013	5	4420 - 4470	2012-10-14	13:10:24	60	Corryvreckan				
DAT_013	6	5040 - 5100	2012-10-14	13:20:44	58	Corryvreckan				
DAT_013	7	5690 - 5750	2012-10-14	13:31:34	60	Corryvreckan				
DAT_013	8	6590 - 6700	2012-10-14	13:46:34	97	Corryvreckan				
DAT_013	9	7400 - 7520	2012-10-14	14:00:04	94	Corryvreckan				
DAT_013	10	7700 - 7780	2012-10-14	14:05:04	73	Corryvreckan				

— End of Document —